6. Oshima M, Dinchuk JE, Kargman SL, et al. Suppression of intestinal polyposis in *Apc*$^{\Delta 716}$ knockout mice by inhibition of cyclooxygenase 2 (COX-2). Cell 1996;87:803–809.
7. Gupta RA, DuBois RN. Colorectal cancer prevention and treatment by inhibition of cyclooxygenase-2. Nat Rev Cancer 2001;1:11–21.
8. Sonoshita M, Takaku K, Sasaki N, et al. Acceleration of intestinal polyposis through prostaglandin receptor EP2 in *Apc*$^{\Delta 716}$ knockout mice. Nat Med 2001;7:1048–1051.
9. Wang D, Wang H, Shi Q, et al. Prostaglandin $E_2$ promotes colorectal adenoma growth via transactivation of the nuclear peroxisome proliferators-activated receptor δ. Cancer Cell 2004;6:285–295.
10. Buchanan F, Gorden DL, Matta P, et al. Role of β-arrestin 1 in the metastatic progression of colorectal cancer. Proc Natl Acad Sci U S A 2006;103:1492–1497.
11. Saukkonen K, Rintahaka J, Sivula A, et al. Cyclooxygenase-2 and gastric carcinogenesis. APMIS 2003;111:915–925.
12. Sun WH, Yu Q, Shen H, et al. Roles of *Helicobacter pylori* infection and cyclooxygenase-2 expression in gastric carcinogenesis. World J Gastroenterology 2004;10:2809–2813.
13. Oshima H, Oshima M, Inaba T, et al. Hyperplastic gastric tumors induced by activated macrophages in COX-2/mPGES-1 transgenic mice. EMBO J 2004;23:1669–1678.
14. Qian BZ, Pollard JW. Macrophage diversity enhances tumor progression and metastasis. Cell 2010;141:39–51.
15. Oshima H, Matsunaga A, Fujimura T, et al. Carcinogenesis in mouse stomach by simultaneous activation of the Wnt signaling and prostaglandin $E_2$ pathway. Gastroenterology 2006;131:1086–1095.
16. Rakoff-Nahoum S, Paglino J, Eslami-Varzaneh F, et al. Recognition of commensal microflora by Toll-like receptors is required for intestinal homeostasis. Cell 2004;118:229–241.
17. Lee CW, Rickman B, Rogers AB, et al. Combination of sulindac and antimicrobial eradication of *Helicobacter pylori* prevents progression of gastric cancer in hypergastrinemic INS-GAS mice. Cancer Res 2009;69:8166–8174.
18. Takeuchi K, Tanaka A, Kato S, et al. Effect of (S)-4-(1-(5-Chloro-2-(4-fluorophenyoxy)benzamido)ethyl) benzoic acid (CJ-42794), a selective antagonist of prostaglandin E receptor subtype 4, on ulcerogenic and healing responses in rat gastrointestinal mucosa. J Pharmacol Exp Ther 2007;322:903–912.
19. Kaparakis M, Walduck AK, Price JD, et al. Macrophages are mediators of gastritis in acute *Helicobacter pylori* infection in C57BL/6 mice. Infect Immun 2008;76:2235–2239.
20. van Rooijen N, Sanders A. Liposome mediated depletion of macrophages: mechanism of action, preparation of liposomes and applications. J Immunol Methods 1994;174:83–93.
21. Oshima H, Itadani H, Kotani H, et al. Induction of prostaglandin $E_2$ pathway promotes gastric hamartoma development with suppression of bone morphogenetic protein signaling. Cancer Res 2009;69:2729–2733.
22. Popivanova BK, Kostadinova FI, Furuichi K, et al. Blockade of a chemokine, CCL2, reduces chronic colitis-associated carcinogenesis in mice. Cancer Res 2009;69:7884–7892.
23. Mantovani A, Sozzani S, Locati M, et al. Macrophage polarization: tumor-associated macrophages as a paradigm for polarized M2 mononuclear phagocytes. TRENDS Immunol 2002;23:549–555.
24. DeNardo DG, Barreto JB, Andreu P, et al. $CD4^+$ T cell regulates pulmonary metastasis of mammary carcinomas by enhancing protumor properties of macrophages. Cancer Cell 2009;16:91–102.
25. Oguma K, Oshima H, Aoki M, et al. Activated macrophages promote Wnt signaling through tumour necrosis factor-α in gastric tumour cells.EMBO J 2008;27:1671–1681.
26. Greten FR, Eckmann, L, Greten TF, et al. IKKβ links inflammation and tumorigenesis in a mouse model of colitis-associated cancer. Cell 2004;118:285–296.
27. Pull SL, Doherty JM, Mills JC, et al. Activated macrophages are an adaptive element of the colonic epithelial progenitor niche necessary for regenerative responses to injury. Proc Natl Acad Sci U S A 2005;102:99–104.
28. Roth KA, Kapadia SB, Martin SM, et al. Cellular immune responses are essential for the development of *Helicobacter felis*-associated gastric pathology. J Immunol 1999;163:1490–1497.
29. Oshima M, Oshima H, Matsunaga A, et al. Hyperplastic gastric tumors with spasmolytic polypeptide-expressing metaplasia caused by tumor necrosis factor-α-dependent inflammation in cyclooxygenase-2/microsomal prostaglandin E sunthase-1 transgenic mice. Cancer Res 2005;65:9147–9151.
30. Li Q, Ishikawa TO, Oshima M, et al. The threshold level of adenomatous polyposis coli protein for mouse intestinal tumorigenesis. Cancer Res 2005;65:8622–8627.
31. Fodde R, Brabletz T. Wnt/β-catenin signaling in cancer stemness and malignant behavior. Curr Opin Cell Biol 2007;19,150–158.
32. Meyer F, Ramanujam KS, Gobert AP, et al. Cutting edge: cyclooxygenase-2 activation suppresses Th1 polarization in response to *Helicobacter pylori*. J Immunol 2003;171:3913–3917.


**Received December 3, 2009. Accepted November 3, 2010.**

***Reprint requests***

**Address requests for reprints to: Masanobu Oshima, DVM, PhD, Division of Genetics, Cancer Research Institute, Kanazawa University, Kakuma-machi, Kanazawa, 920-1192 Japan. e-mail: oshimam@kenroku.kanazawa-u.ac.jp;fax: (81) 76-234-4519.**

***Acknowledgments***

**The authors thank Manami Watanabe for her excellent technical assistance.**

**K.O. is a Research Fellow of the Japan Society for the Promotion of Science, Japan.**

***Conflicts of interest***

**The authors disclose no conflicts.**

***Funding***

**Supported by Grants-in-Aid from the Ministry of Education, Culture, Sports, Science and Technology of Japan and the Ministry of Health, Labour and Welfare of Japan.**

## Supplementary Materials and Methods

### *Depletion of Indigenous Bacteria*

To deplete indigenous bacteria in the stomach, specific pathogen free (SPF)-*Gan* (*Gan* for Gastric neoplasia) mice (n = 5) were administered ampicillin (1 g/L; Sigma, St. Louis, MO), vancomycin (500 mg/L; Sigma), neomycin sulfate (1 g/L; Sigma), and metronidazole (1g/L; Sigma) in drinking water as previously described.[1] Gastric tumors were examined by x-ray computerized tomography using a LaTheta LCT-100 instrument (Aloka, Tokyo, Japan) after 0, 2, and 4 weeks of antibiotic administration. The mean tumor area was calculated from computerized tomography images using a National Institute of Health (NIH) Image J software program (Bethesda, MD).

### *Histology and Immunohistochemistry*

Stomach tissue specimens were fixed in 4% paraformaldehyde, paraffin-embedded, and sectioned at 4-$\mu$m thickness. Frozen sections were used for CD4 immunostaining. The construction of SPF-*Rag2*$^{-/-}$*K19-C2mE* mice was described previously.[2] Antibodies for $\beta$-catenin (Sigma), mannose receptor (AbD Serotec, Raleigh, NC), CD3$\varepsilon$ (Santa Cruz Biotechnology, Santa Cruz, CA), and CD4 (BD Pharmingen, Columbus, NE) were used as the primary antibodies. Alexa Fluor 594 or Alexa Fluor 488 antibody (Molecular Probes, Eugene, OR) was used as the secondary antibody. Infection of *Helicobacter felis* in the gastric glands was confirmed using hematoxyin-stained paraffin sections of the *H felis*-infected germfree-*Gan* mouse stomach at $\times$1000 magnification.

### *Expression Analysis of M2 Macrophage Markers*

The expression profiles of M2 macrophage markers Ym1, Ym2, arginase 1 (Arg1), and transforming growth factor-$\beta$1 in *Gan*, *K19-C2mE*, and wild-type mouse stomachs were downloaded from the National Center for Biotechnology Information Gene Expression Omnibus (GEO; accession number GSE16902). These expression data were transformed to log10 ratios to the average of wild-type mouse samples.

### References

1. Rakoff-Nahoum S, Paglino J, Eslami-Varzaneh F, et al. Recognition of commensal microflora by Toll-like receptors is required for intestinal homeostasis. Cell 2004;118:229–241.
2. Oshima M, Oshima H, Matsunaga A, et al. Hyperplastic gastric tumors with spasmolytic polypeptide-expressing metaplasia caused by tumor necrosis factor-$\alpha$-dependent inflammation in cyclooxygenase-2/microsomal prostaglandin E sunthase-1 transgenic mice. Cancer Res 2005;65:9147–9151.
3. Oshima H, Matsunaga A, Fujimura T, et al. Carcinogenesis in mouse stomach by simultaneous activation of the Wnt signaling and prostaglandin $E_2$ pathway. Gastroenterology 2006;131:1086–1095.
4. Oshima H, Oshima M, Inaba T, et al. Hyperplastic gastric tumors induced by activated macrophages in COX-2/mPGES-1 transgenic mice. EMBO J 2004;23:1669–1678.

**Supplementary Table 1.** Genotypes and Phenotypes of Transgenic Mouse Models

| Strain name | Transgene(s) | Phenotypes in the glandular stomach (reference) |
|---|---|---|
| *K19-Wnt1* | *Wnt1* | Activation of canonical Wnt signaling<br>Small preneoplastic lesions consisting of Wnt-promoted epithelial cells with macrophage infiltration and activation.[3] |
| *K19-C2mE* | *Ptgs2* and *Ptges*, encoding COX-2 and mPGES-1, respectively | Activation of $PGE_2$ pathway<br>Hyperplasia consisting of TFF2-positive metaplastic mucous cells associated with inflammatory infiltration.[2,4] |
| *K19-Wnt1/C2mE* (*Gan* for Gastric neoplasia) | *Wnt1*, *Ptgs2*, and *Ptges* | Activation of both Wnt and $PGE_2$ pathways<br>Development of dysplastic tumors with the infiltration of macrophages.[3] |

$PGE_2$, prostaglandin $E_2$; COX-2, cyclooxygenase-2; *Ptgs2*, gene symbol for mouse COX-2; mPGES-1, microsomal prostaglandin E synthase-1; *Ptges*, gene symbol for mouse mPGES-1; TFF2, trefoil factor 2.

**Supplementary Table 2.** Results of Germfree Monitoring Tests

| Samples | Feces | | | Bedding | | | Swab | |
|---|---|---|---|---|---|---|---|---|
| Media | TGC[a] | | PDB[b] | TGC | | PDB | PDB | |
| Temp[c] | 37 | RT | RT | 37 | RT | RT | RT | Fecal smear |
| Mouse age, wks | | | | | | | | |
| 2 | — | — | — | — | — | — | — | — |
| 3 | — | — | — | — | — | — | — | — |
| 5 | — | — | — | — | — | — | — | — |
| 10 | — | — | — | — | — | — | — | — |
| 15 | — | — | — | — | — | — | — | — |
| 20 | — | — | — | — | — | — | — | — |
| 23 | — | — | — | — | — | — | — | — |
| 28 | — | — | — | — | — | — | — | — |
| 31 | — | — | — | — | — | — | — | — |
| 45 | — | — | — | — | — | — | — | — |
| 50 | — | — | — | — | — | — | — | — |
| 55 | — | — | — | — | — | — | — | — |

RT, room temperature; Temp, temperature.
[a]Thioglycollate medium.
[b]Potato dextrose broth.
[c]Samples were incubated in TGC at 37°C or at room temperature or in PDB at room temperature.

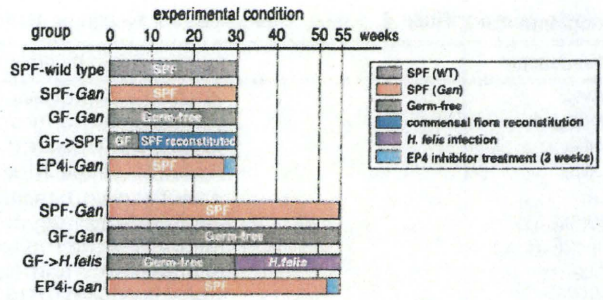


**Supplementary Figure 1.** A schematic illustration of the experimental schedule. The gastric phenotypes of specific pathogen free (SPF)-*Gan* and germfree (GF)-*Gan* mice were examined at 30 and 55 weeks of age. GF-*Gan* mice were reconstituted with commensal flora at 7 weeks of age, and gastric phenotypes were examined at 30 weeks of age. The EP4 inhibitor was administered for 3 weeks from 27 or 52 weeks of age. GF-*Gan* mice were infected with *Helicobacter felis* at 30 weeks of age, and infected mice were examined at 55 weeks of age.

**Supplementary Table 3.** List of Excluded Pathogens in Animal Room 4 of SPF Facility, Kanazawa University

| |
|---|
| *Bordetella bronchiseptica* |
| *Citrobacter rodentium* |
| *Corynebacterium kutscheri* |
| *Mycoplasma pulmonis* |
| *Pasteurella pneumotropica* |
| *Salmonella* spp |
| *Streptococcus pneumoniae* |
| *Pseudomonas aeruginosa* |
| *Helicobacter hepaticus* |
| *Clostridium piliforme* |
| Ectromelia virus |
| Sialodacryoadenitis virus (SDAV) |
| Hanta virus |
| Lymphocytic choriomeningitis virus (LCMV) |
| Mouse hepatitis virus |
| Sendai virus |
| Intestinal protozoas (*Giardia muris, Spironucleus muris, Tritrichomonas muris, Octomitus pulcher,* Coccidiosis) |
| Helminths (*Aspiculuris tetraptera, Syphacia obvelata*) |
| Parasites (*Myobia* sp, *Polyplaxserrata*) |

NOTE. All SPF mice used in the present study were raised in this SPF room.
SPF, specific antigen free.

**Supplementary Table 4.** Primer Sequences for Real-time RT-PCR

| Gene name | Forward primer | Reverse primer |
|---|---|---|
| COX-2 | GTGTGCGACATACTCAAGCAGGA | TGAAGTGGTAACCGCTCAGGTG |
| mPGES-1 | CTGCAGCACACTGCTGGTCA | CTCCACATCTGGGTCACTCCTGTA |
| TNF-$\alpha$ | AAGCCTGTAGCCCACGTCGTA | GGCACCACTAGTTGGTTGTCTTTG |
| IL-1$\beta$ | TCCAGGATGAGGACATGAGCAC | GAACGTCACACACCAGCAGGTTA |
| IL-6 | CCACTTCACAAGTCGGAGGCTTA | GCAAGTGCATCATCGTTGTTCATAC |
| KC(CXCL1) | GCTTGAAGGTGTTGCCCTCAG | AAGCCTCGCGACCATTCTTG |
| MIP-2(CXCL2) | GCGCTGTCAATGCCTGAAGA | TTTGACCGCCCTTGAGAGTG |
| CCL2 | GCATCCACGTGTTGGCTCA | CTCCAGCCTACTCATTGGGATCA |
| CCL3 | TGAAACCAGCAGCCTTTGCTC | AGGCATTCAGTTCCAGGTCAGTG |
| CCL4 | CCATGAAGCTCTGCGTGTCTG | GGCTTGGAGCAAAGACTGCTG |
| CCL5 | ACCAGCAGCAAGTGCTCCAA | TGGCTAGGACTAGAGCAAGCAATG |
| CCL7 | GCATCCACATGCTGCTATGTCA | GATGGGCTTCAGCACAGACTTC |
| CCL8 | TGCCTGCTGCTCATAGCTGTC | GACATACCCTGCTTGGTCTGGAA |
| EP4 | GTGGTGCTCATCTGCTCCATTC | CTGCAAATCTGGGTTTCTGCTG |
| CD44 | TTTAACCTATATGCAGCAAGCCACT | CAGAATCATCACCACTATGGCAAG |
| EphB3 | AGCTGTGAATATCACCACCAACCA | TGACTCCATTAGGCCGCTCTG |

COX-2, cyclooxygenase-2; IL-1$\beta$, interleukin-1$\beta$; IL-6, interleukin-6; mPGES-1, microsomal prostaglandin E synthase-1; RT-PCR, reverse-transcription polymerase chain reaction; TNF-$\alpha$, tumor necrosis factor-$\alpha$; KC, keratinocyte-derived chemokine; MIP-2, macrophage inflammatory protein-2; CXCL, chemokine (C-X-C motif) ligand; CCL, chemokine (C-C motif) ligand; EP4, PGE$_2$ receptor subtype 4; EphB3, Eph receptor B3.

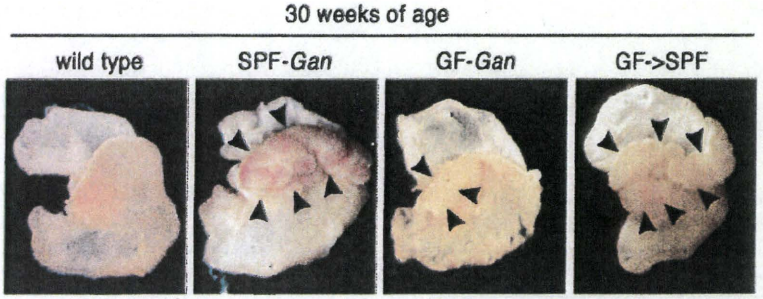


**Supplementary Figure 2.** Representative photographs of gastric tumor phenotypes at 30 weeks of age. Wild-type mouse stomach, gastric tumors of SPF-*Gan* mouse, GF-*Gan* mouse, and GF-*Gan* mouse reconstituted with commensal bacteria (GF->SPF) are shown (from left to right). *Arrowheads* indicate gastric tumors in SPF-*Gan*, GF-*Gan*, and GF->SPF *Gan* mice.

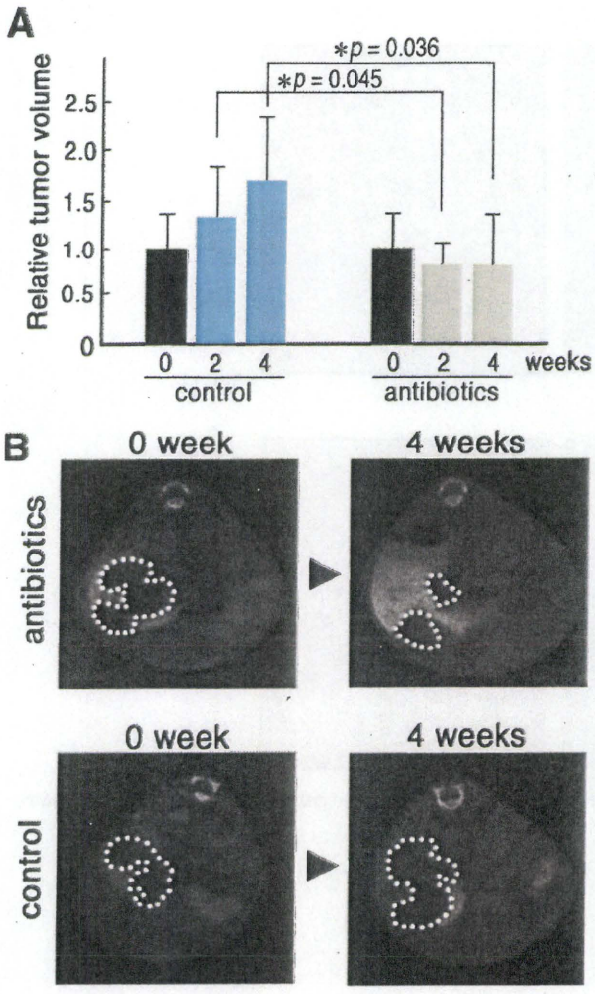


**Supplementary Figure 3.** Suppression of gastric tumor growth by antibiotic treatment. (*A*) The mean tumor volumes calculated from x-ray computerized tomography (CT) images of control *Gan* mice (*blue bars*, *left*) and antibiotics-treated *Gan* mice (*green bars*, *right*) relative to the level at 0 weeks of treatment (*closed bars*) (mean ± standard deviation). *$P < .05$. (*B*) Representative x-ray CT images of gastric tumors of the same mice from the antibiotics-treated group (*top*) and control group (*bottom*) at 0 and 4 weeks of antibiotic treatment. The *dashed lines* indicate gastric tumors. Note that tumor growth was suppressed by treatment with antibiotics (*top*).

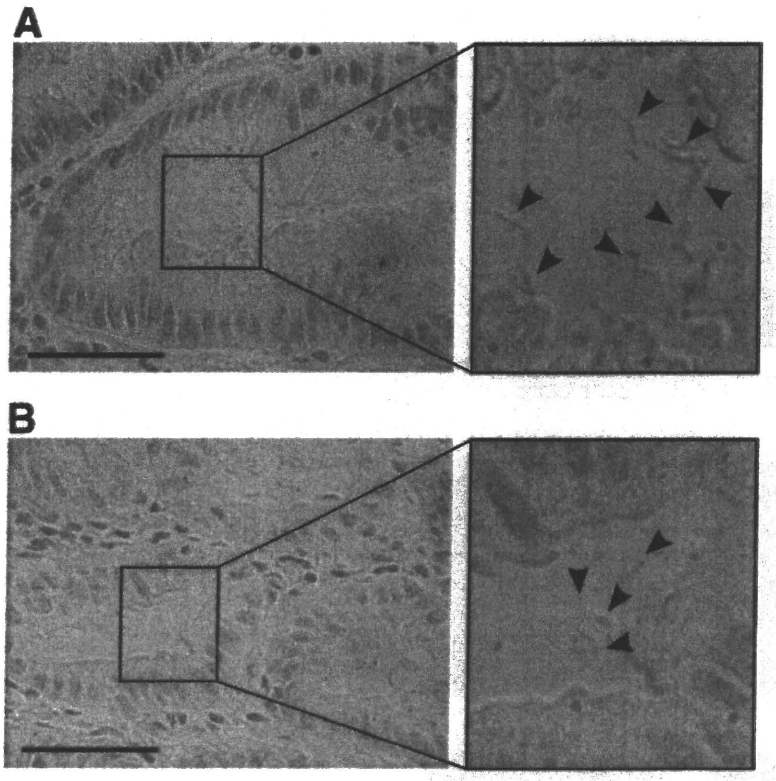


**Supplementary Figure 4.** Infection of *Helicobacter felis* in the lumen of the *H felis*-infected GF-*Gan* mouse gastric glands (*A* and *B*). *Arrowheads* indicate *H felis*. *Scale bars*, 50 μm. Original magnification, ×1000.

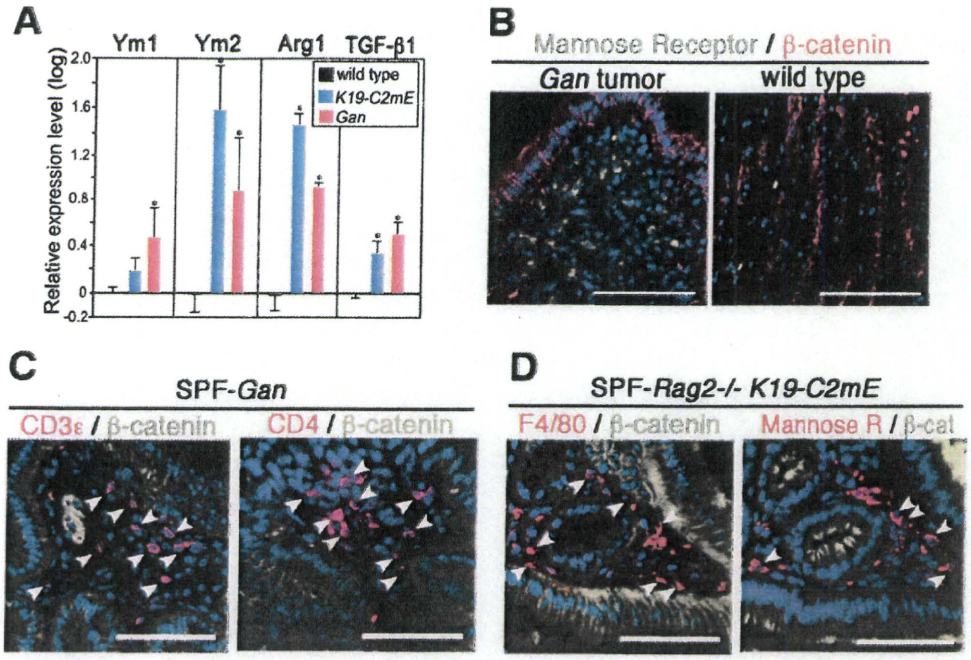


**Supplementary Figure 5.** M2 macrophages in *Gan* and *K19-C2mE* mouse stomachs. (*A*) The relative expression level of M2 macrophage markers—Ym1, Ym2, arginase 1 (Arg1), and transforming growth factor (TGF)-β1—in the *K19-C2mE* mouse stomach (*blue*) and *Gan* mouse tumors (*red*) in comparison with that in the wild-type mouse stomach (*black*) (mean log10 ratio with standard deviation). *$P < .05$ vs wild-type level. (*B*) Immunostaining of M2 macrophage marker, mannose receptor (*green*) and β-catenin (*red*) with 4′,6-diamidino-2-phenylindole (DAPI) nuclear staining (*blue*) in *Gan* mouse tumors (*left*) and wild-type mouse stomach (*right*). (*C*) Immunostaining of CD3ε (*left, red, arrowheads*) or CD4 (*right, red, arrowheads*) and β-catenin (*green*) with DAPI staining (*blue*) of SPF-*Gan* mouse tumors. (*D*) Immunostaining of F4/80 (*left, red, arrowheads*) or mannose receptor (*right, red, arrowheads*) and β-catenin (*green*) with DAPI staining (*blue*) of the SPF-*Rag2*$^{-/-}$ *K19-C2mE* mouse stomach. Note that mannose receptor-expressing M2 macrophages were found in the T cell-depleted Rag2$^{-/-}$ *K19-C2mE* mouse inflamed stomach. *Scale bars* in *B–D*, 100 μm.

Cancer Science
The official journal of the Japanese Cancer Association JCA

# Activation of epidermal growth factor receptor signaling by the prostaglandin $E_2$ receptor EP4 pathway during gastric tumorigenesis

Hiroko Oshima, Boryana K. Popivanova, Keisuke Oguma,[2] Dan Kong, Tomo-o Ishikawa and Masanobu Oshima[1]

Division of Genetics, Cancer Research Institute, Kanazawa University, Kanazawa, Japan

(Received August 11, 2010/Revised December 9, 2010/Accepted December 22, 2010/Accepted manuscript online January 4, 2011/Article first published online February 2, 2011)

**Cyclooxygenase-2 (COX-2) plays an important role in tumorigenesis through prostaglandin $E_2$ ($PGE_2$) biosynthesis. It has been shown by *in vitro* studies that $PGE_2$ signaling transactivates epidermal growth factor receptor (EGFR) through an intracellular mechanism. However, the mechanisms underlying $PGE_2$-induced EGFR activation in *in vivo* tumors are still not fully understood. We previously constructed transgenic mice that develop gastric tumors caused by oncogenic activation and $PGE_2$ pathway induction. Importantly, expression of EGFR ligands, epiregulin, amphiregulin, heparin-binding EGF-like growth factor, and betacellulin, as well as a disintegrin and metalloproteinases (ADAMs), ADAM8, ADAM9, ADAM10, and ADAM17 were significantly increased in the mouse gastric tumors in a $PGE_2$ pathway-dependent manner. These ADAMs can activate EGFR by ectodomain shedding of EGFR ligands. Notably, the extensive induction of EGFR ligands and ADAMs was suppressed by inhibition of the $PGE_2$ receptor EP4. Moreover, EP4 signaling induced expression of amphiregulin and epiregulin in activated macrophages, whereas EP4 pathway was required for basal expression of epiregulin in gastric epithelial cells. In contrast, ADAMs were not induced directly by $PGE_2$ in these cells, suggesting indirect mechanism possibly through $PGE_2$-associated inflammatory responses. These results suggest that $PGE_2$ signaling through EP4 activates EGFR in gastric tumors through global induction of EGFR ligands and ADAMs in several cell types either by direct or indirect mechanism. Importantly, gastric tumorigenesis of the transgenic mice was significantly suppressed by combination treatment with EGFR and COX-2 inhibitors. Therefore, it is possible that inhibition of both COX-2/$PGE_2$ and EGFR pathways represents an effective strategy for preventing gastric cancer. (*Cancer Sci* 2011; 102: 713–719)**

It has been established that induction of cyclooxygenase 2 (COX-2) plays an important role in cancer development.[1,2] Genetic mouse model studies indicated that prostaglandin $E_2$ ($PGE_2$), a downstream products of COX-2, plays a key role in intestinal tumorigenesis,[3–5] suggesting that the $PGE_2$ pathway is a possible target for the chemoprevention. On the other hand, epidermal growth factor receptor (EGFR) signaling is also an important target for cancer prevention.[6] Inhibition of EGFR signaling in $Apc^{Min}$ mice, a model of familial adenomatous polyposis, significantly suppresses intestinal polyposis.[7–9] Importantly, combination treatment using an EGFR inhibitor with non-steroidal anti-inflammatory drugs or a COX-2 inhibitor dramatically suppresses intestinal tumorigenesis.[8,9] It has been shown by *in vitro* experiments that $PGE_2$ signaling transactivates EGFR through activation of cSrc[10,11] or MMPs[12], as well as induction of amphiregulin, an EGFR ligand[13,14] or tumor necrosis factor-α converting enzyme/a disintegrin and metalloproteinase 17 (TACE/ADAM17), a shedding enzyme for amphiregulin.[15] However, the mechanism responsible for the activation of EGFR by the $PGE_2$ pathway in *in vivo* tumors has not been fully elucidated. Induction of the $PGE_2$ pathway in the gastric mucosa causes development of inflammatory microenvironment consisting of macrophages and myofibroblasts.[16,17] It is therefore possible that $PGE_2$ signaling in such microenvironment contributes to EGFR activation in tumors, and that $PGE_2$-associated inflammatory responses are also involved in EGFR activation.

Gastric cancer is one of the most frequently diagnosed and lethal malignancies worldwide, with a 5-year survival of only about 20%.[18] COX-2 expression is induced in more than 70% of gastric cancers,[19] and regular use of non-steroidal anti-inflammatory drugs decreases the risk of gastric cancer.[20] suggesting a role of COX-2 pathway in gastric tumorigenesis. In addition to COX-2, activation of Wnt signaling is found in 30–50% of gastric cancers.[21,22] Based on these results, we constructed *K19-Wnt1/C2mE* transgenic mice expressing *Wnt1*, *Ptgs2*, and *Ptges* encoding Wnt1, COX-2, and microsomal prostaglandin E synthase-1, respectively, in gastric mucosa.[22] *K19-Wnt1/C2mE* mice (*Gan* mice for gastric neoplasia) develop gastric tumors caused by the simultaneous activation of Wnt and $PGE_2$ pathways, although Wnt activation alone results in the development of only small dysplastic lesions. Gene expression profiles of *Gan* mouse tumors were similar to those of human intestinal-type gastric cancer.[23] We also constructed *K19-Nog/C2mE* transgenic mice that express *Nog* encoding noggin, together with *Ptgs2* and *Ptges*.[24] Noggin is an endogenous antagonist for bone morphogenetic protein signaling. *K19-Nog/C2mE* mice develop gastric hamartomas, although *Nog* expression alone does not cause any morphological changes. These results indicate that induction of the $PGE_2$ pathway plays a key role in the promotion of gastric tumorigenesis, regardless of the types of underlying oncogenic pathway such as Wnt activation or bone morphogenetic protein suppression.[25]

Using these mouse models, we have investigated the mechanism of EGFR activation by the $PGE_2$ pathway in gastric tumorigenesis. We also examined the role of EGFR signaling in the *in vivo* tumor development by drug dosing experiments.

## Materials and Methods

**Mouse models.** Construction of *K19-Wnt1*, *K19-C2mE*, *K19-Nog*, *K19-Wnt1/C2mE* (*Gan*), and *K19-Nog/C2mE* mice was described previously.[25] Briefly, both *Ptgs2* and *Ptges* are expressed in the *K19-C2mE* mouse stomach, whereas *Wnt1* and *Nog* are expressed in *K19-Wnt1* and *K19-Nog* mice, respectively. Expression of these genes is regulated by the *Krt19* gene promoter that is transcriptionally active in gastric epithelial cells. *Gan* mice and *K19-Nog/C2mE* mice were obtained by

[1]To whom correspondence should be addressed.
E-mail: oshimam@kenroku.kanazawa-u.ac.jp
[2]Research fellow of the Japan Society for the Promotion of Science.

doi: 10.1111/j.1349-7006.2011.01847.x

**Table 1. Transgenic mouse models and their gastric phenotypes**

| Transgenic mice | Transgenes | Affected pathway(s) | Gastric phenotype (reference) |
|---|---|---|---|
| *K19-C2mE* | *Ptgs2, Ptges* | $PGE_2$ induction | Inflammation, hyperplasia[16,25] |
| *K19-Wnt1* | *Wnt1* | Wnt activation | Small dysplastic lesion[22,25] |
| *K19-Nog* | *Nog* | BMP suppression | No phenotype[24,25] |
| *K19-Wnt1/C2mE (Gan)* | *Wnt1, Ptgs2, Ptges* | Wnt activation/$PGE_2$ induction | Dysplastic tumor[22,25] |
| *K19-Nog/C2mE* | *Nog, Ptgs2, Ptges* | BMP suppression/$PGE_2$ induction | Hamartoma[24,25] |

BMP, bone morphogenetic protein.

crossing *K19-C2mE* with *K19-Wnt1* or *K19-Nog*, respectively (Table 1). All animal experiments were carried out according to a protocol approved by the Committee on Animal Experimentation of Kanazawa University.

**Microarray analyses.** We have deposited the results of microarray data sets from a series of mouse models to the Gene Expression Omnibus, as accession GSE16902.[23] Expression profiles of EGFR ligands, EGFR family members, and ADAM family proteases were extracted from the data sets, and the expression levels were compared by using absolute values.

**Drug administration.** For inhibition of COX-2, mice were fed a diet containing celecoxib (Pfizer New York, NY, USA) at 1500 ppm. For inhibition of EGFR or EP4 receptor, mice were administered orally with ZD1839 (Astra Zeneca, London, UK) or RQ00015986/CJ-42794[26] (RaQualia, Taketoyo, Japan), respectively, at 100 mg/kg/day in 0.5% methylcellulose. Drug-dosing experiments using *Gan* mice were performed for 3 weeks from 47 weeks of age ($n = 5$ for each experiment). The relative gastric tumor volume was calculated by multiplication of tumor height and tumor area measured using the ImageJ application program (NIH, Bethesda, MD, USA). X-ray computed tomography images of gastric tumors in live mice were examined using LaTheta LCT-100 (Aloka, Tokyo, Japan) at weeks 0, 1, 2 and 3 of drug administration.

**Reverse transcription-polymerase chain reaction.** Total RNA was extracted from mouse stomach or cultured cells using ISOGEN (Nippon Gene, Tokyo, Japan). Extracted RNA was reverse-transcribed with a PrimeScript RT reagent kit (Takara, Tokyo, Japan) and PCR-amplified by ABI prism 7900HT (Applied Biosystems, Carlsbad, CA, USA) using SYBR Premix Ex Taq II (Takara). Primers for real-time RT-PCR were purchased (Takara).

**Cell Culture experiments.** Mouse macrophage RAW264 cells (RIKEN BioRessource Center, Tsukuba, Japan) were cultured in RPMI1640, and treated with lipopolysaccharide (LPS) (Sigma, St. Louis, MO, USA) at 100 ng/mL with or without treatment of celecoxib or RQ00015986 at 10 μM for 24 h. Medium concentration of amphiregulin was measured by using Mouse Amphiregulin ELISA kit (RayBiotech, Norcross, GA, USA). Knockdown of *Adam8* expression was performed using *Adam8* ON-TARGETplus SMARTpool siRNA reagents (Dharmacon, Boulder, CO, USA). For the primary culture of gastric epithelial cells, glandular stomachs of *K19-Wnt1* mice were treated with 0.1% collagenase for 45 min followed by trypsin digestion, and cells were cultured in matrigel (BD Biosciences, Franklin Lakes, NJ, USA) with the primary culture medium with or without 1 μg/mL EGF (BD Biosciences)[16] supplemented with 500 ng/mL R-spondin1 (R&D, Mineapolis, MN, USA), 1 μM of Jagged1 (AnaSpec, Fremont, CA, USA), and 100 ng/mL of Noggin (PeproTech, Rocky Hill, NJ, USA). The primary cultured cells were stimulated with mouse recombinant amphiregulin and epiregulin (R&D) at 20 and 1 ng/mL, respectively, and the mean number of cystic structures >75 μm in diameter per microscopic field was calculated at day 5.

**Immunoblotting analysis.** Tissue samples were homogenized and sonicated in lysis buffer. After centrifugation at 2000*g*, 10 μg of the supernatant protein was separated in a 10% SDS-polyacrylamide gel. Antibodies for phosphorylated Akt (Ser473) and phosphorylated p44/42 Erk1/2 (cell signaling) were used as the primary antibodies. β-Actin was used as an internal control. The ECL detection system (GE Healthcare, Buckinghamshire, UK) was used to detect specific signals. The band intensities were measured using the ImageJ application (NIH).

**Histology and immunohistochemistry.** Tissues and the primary cultured cells were paraffin-embedded or frozen in OCT compound (Sakura Finetechnical, Tokyo, Japan), and sectioned. These sections were stained with H&E or processed for immunostaining. Antibody for phosphorylated EGFR (Tyr845) (cell signaling), Ki-67 (DakoCytomation, Carpenteria, CA, USA), or active β-catenin (Millipore, Billerica, MA, USA) was used as the primary antibody. Immunostaining signals were visualized using the Vectastain Elite kit (Vector Laboratories, Burlingame, CA, USA). For fluorescence immunostaining, anti-rabbit IgG Alexa 488 (Molecular Probes, Eugene, OR, USA) was used for the secondary antibody. The mean Ki-67 labeling index of the five independent microscopic fields was calculated.

**Statistical analysis.** Statistical analyses were performed using the unpaired Student's *t*-test, with *P*-values <0.05 considered significant.

## Results

**Induction of EGFR ligands and ADAM proteases in gastric tumors by $PGE_2$ pathway.** We examined gene expression profiles of EGFR ligands and EGFR members in the stomach or gastric tumors of the all mouse models listed in Table 1. Among these models, $PGE_2$ pathway is induced in the stomach of *K19-C2mE*, *Gan*, and *K19-Nog/C2mE* mice by expression of *Ptgs2* and *Ptges*. Hereafter, these three strains are termed the *C2mE* group. Interestingly, expression of amphiregulin (*Areg*), epiregulin (*Ereg*), HB-EGF (*Hbegf*), and betacellulin (*Btc*), as well as Her2 (*Erbb2*), and Her3 (*Erbb3*) increased significantly in the stomach of the *C2mE* group mice (Fig. 1a). In contrast, such induction was not observed in the stomach of *K19-Wnt1* and *K19-Nog* mice, indicating that induction of $PGE_2$ pathway is responsible for upregulation of these genes.

ADAMs activate EGFR signaling through ectodomain shedding of EGFR ligands, and are induced in a variety of cancer tissues.[27] Notably, expression of *Adam8*, *Adam9*, *Adam10*, *Adam17*, and *Adam28* was increased significantly in the stomach of the *C2mE* group mice but not in other strains, indicating the $PGE_2$ pathway-dependent induction of these ADAMs (Fig. 1b). It has been shown that ADAM8, ADAM 10 and ADAM17 can cleave and activate amphiregulin, epiregulin, HB-EGF, or betacellulin.[28–30] It is thus possible that EGFR is activated in the gastric mucosa of *C2mE* group mice through induction of both EGFR ligands and ADAM proteases. Induction of *Erbb2* may also contribute to EGFR activation by increasing the heterodimerization of EGFR and HER2. Consistently, the immunostaining intensity of phosphorylated EGFR increased significantly in the gastric epithelial cells of *K19-C2mE* and *Gan* mice but not in those of WT and *K19-Wnt1* mice, indicating $PGE_2$ pathway-dependent EGFR activation (Fig. 1c).



doi: 10.1111/j.1349-7006.2011.01847.x

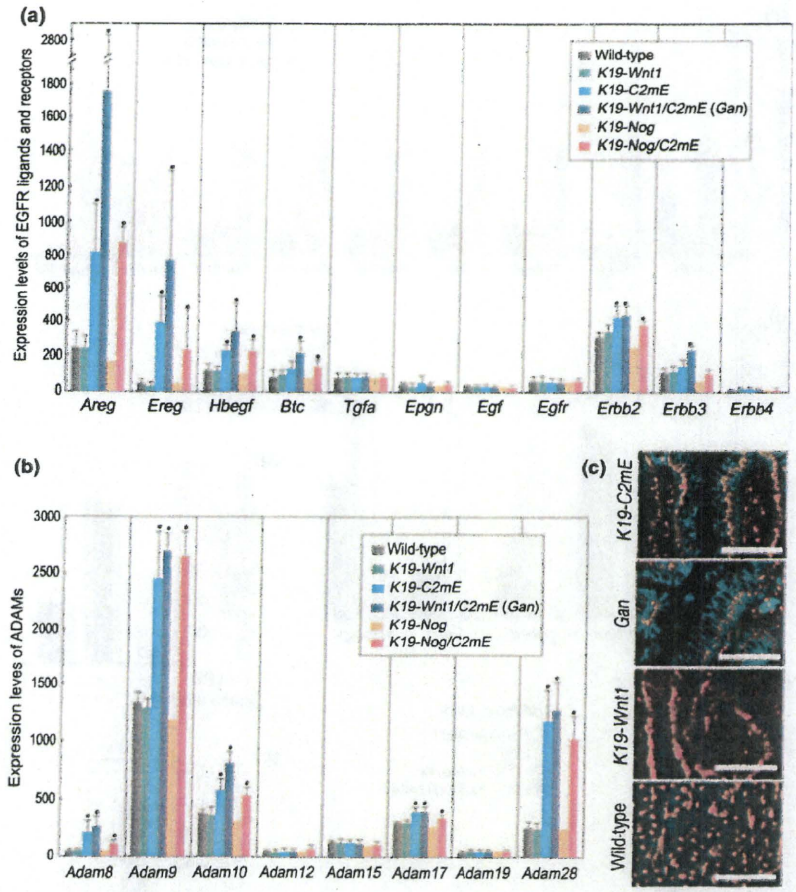


**Fig. 1.** Gene expression levels of epidermal growth factor receptor (EGFR) ligands, EGFR family members (a) and a disintegrin and metalloproteinases (ADAMs) (b) in the stomach of the respective models (mean ± SD) calculated from microarray results. Asterisks indicate $P < 0.05$ versus the wild-type level. (c) Fluorescence immunostaining for phosphorylated EGFR at Tyr845 (green) in the gastric mucosa of the indicated genotype mice. DAPI staining for nuclei is visualized in red. Bars indicate 100 μm.

**Induction of EGFR ligands and ADAM proteases by $PGE_2$ receptor EP4 signaling.** We next treated *Gan* mice with a COX-2 inhibitor, celecoxib, and found that expression of *Areg*, *Ereg*, *Hbegf*, and *Btc* as well as *Adam8*, *Adam9*, *Adam10*, *Adam17* and *Adam28* in gastric tumors decreased significantly (Fig. 2a). Among the four $PGE_2$ receptors, EP1-EP4, expression of EP4 was significantly increased in gastric tumors of *C2mE* group mice.[24] We thus treated *Gan* mice with an EP4-specific inhibitor, RQ00015986. Importantly, inhibition of the EP4 receptor caused a decrease in the expression of these EGFR ligands and ADAMs to a similar level to that in the celecoxib-treated mice (Fig. 2a). These results indicate that $PGE_2$ signaling through EP4 is required for induction of EGFR ligands and ADAMs in gastric tumor tissues.

**Induction of EGFR ligands by EP4 signaling in activated macrophages.** Macrophages are infiltrated in the gastric mucosa in the *C2mE* group mice,[16,22] and tumor-associated macrophages play an important role in tumorigenesis through expression of growth factors.[31] We thus examined induction of EGFR ligands and ADAMs in macrophages using the RAW264 cells. Stimulation of macrophages with LPS induced expression of *Ptgs2* and *Ptges*, resulting in an increased $PGE_2$ level in the cell culture medium (Fig. 2b and not shown). In the LPS-activated macrophages, expression of *Areg*, *Ereg*, and *Hbegf*, as well as *Adam8* increased significantly, while expression of other ADAM members did not (Fig. 2b,c). Notably, inhibition of COX-2 or the EP4 receptor by treatment with celecoxib or RQ00015986, respectively, significantly suppressed induction of *Areg* and *Ereg* in the LPS-stimulated macrophages. These results suggest that EP4 signaling induces expression of *Areg* and *Ereg* in the activated macrophages in an autocrine or paracrine manner. In contrast, expression of *Hbegf* and *Adam8* was not decreased by inhibition of COX-2 or EP4, suggesting that other factors from activated macrophages induced these genes. Expression of *Btc* was not detected in the LPS-stimulated or control RAW264 cells (data not shown).

We confirmed that medium concentration of the cleaved amphiregulin increased significantly in the LPS-stimulated RAW264 cells (Fig. 2d). To examine the role of Adam8 in shedding of amphiregulin, we used *Adam8* siRNA that successfully decreased *Adam8* mRNA level in macrophages (Fig. 2e). Importantly, transfection of *Adam8* siRNA reduced amphiregulin concentration significantly (Fig. 2d). These results indicate that LPS stimulation induces amphiregulin secretion from macrophages through induction of *Areg* and *Adam8* in a $PGE_2$-dependent and independent mechanisms.

**Basal epiregulin expression by EP4 signaling in gastric epithelial cells.** To examine gene expression in gastric epithelial cells, we established the primary culture system in matrigel. Although gastric epithelial cells from WT mice proliferated for 3–5 days in matrigel forming small cystic structures (Fig. 3a), they could not continue proliferation. In contrast, gastric epithelial cells from *K19-Wnt1* transgenic mice continued proliferation in matrigel forming large cystic structures. These structures consisted of monolayer of epithelial cells with nuclear accumulation of β-catenin (Fig. 3b), suggesting that Wnt activation increases self-renewal activity of gastric epithelial cells. Expression of EGFR ligands and ADAMs was not increased by $PGE_2$ stimulation in the primary cultured epithelial cells. However, EP4 inhibition resulted in a significant decrease of *Ereg* expression level, suggesting that EP4 signaling is required for basal expression of *Ereg* (Fig. 3c). Expression of *Hbegf* was not detected in the gastric epithelial cells (data not shown).

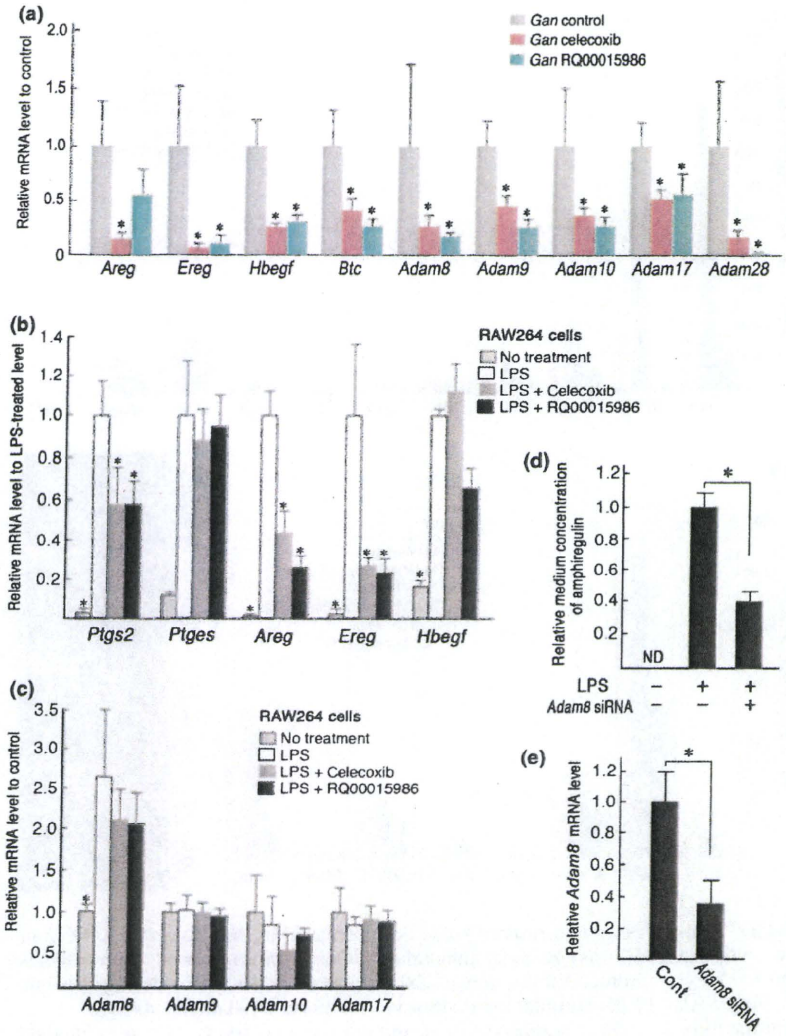


**Fig. 2.** (a) The mRNA levels of epidermal growth factor receptor (EGFR) ligands and a disintegrin and metalloproteinases (ADAMs) examined by real-time RT-PCR in gastric tumors of celecoxib-treated or RQ00015986-treated *Gan* mice relative to the no-drug control *Gan* mouse level (mean ± SD). Asterisks indicate $P < 0.05$ versus the control level. (b) The mRNA levels of *Ptgs2*, *Ptges*, and EGFR ligands in the control and the drug-treated lipopolysaccharide (LPS)-stimulated RAW264 cells relative to that of LPS-stimulated RAW264 cells (mean ± SD). Asterisks indicate $P < 0.05$ versus the level of LPS-stimulated cells. (c) The mRNA levels of *Adams* in no-drug and drug-treated LPS-stimulated RAW264 cells relative to that of control RAW264 cells (mean ± SD). Asterisk indicates $P < 0.05$ versus the level of LPS-stimulated cells. (d) Concentration of amphiregulin in the culture medium of the LPS-stimulated and *Adam8* siRNA-transfected RAW264 cells relative to that of LPS-stimulated RAW264 cells (mean ± SD). Asterisk indicates $P < 0.05$. (e) The *Adam8* mRNA level in the *Adam8* siRNA-transfected RAW264 cells relative to that of control cells (cont) (mean ± SD). Asterisk indicates $P < 0.05$. [Correction added after online publication on March 18, 2011. *Areg* mRNA is changed to *Adam8* on Fig. 2(e).]

Notably, stimulation of the gastric epithelial cells either by amphiregulin or epiregulin increased the size of cystic structures in matrigel, indicating that these EGFR ligands accelerate proliferation of gastric epithelial cells (Fig. 3d). These results support the idea that induction of amphiregulin and epiregulin by $PGE_2$ pathway promotes gastric tumorigenesis through activation of epithelial EGFR.

**Suppression of *Gan* mouse gastric tumorigenesis by EGFR inhibition.** Treatment of *Gan* mice with celecoxib decreased gastric tumor volume to 10.2% of the no-drug control mice, confirming that COX-2 pathway is important for gastric tumorigenesis (Fig. 4a,b). Importantly, treatment of *Gan* mice with an EGFR inhibitor, ZD1839, also reduced the gastric tumor volume to 23.6% of the control mice. Moreover, combination treatment with ZD1839 and celecoxib resulted in complete regression of *Gan* mouse gastric tumors. We confirmed the dramatic regression of gastric tumors by combination therapy with celecoxib and ZD1839 in the same mice by chronological examinations using X-ray computed tomography (Fig. 4c). The transgenic expression of *Ptgs2* and *Wnt1* in the ZD1839-treated *Gan* mice stayed at a similarly high level as that in the control *Gan* mice (Fig. 4d). On the other hand, expression of *Ptges* decreased significantly by ZD1839 treatment, suggesting that endogenous *Ptges* was induced by activation of EGFR signaling in gastric tumors. However, *Ptges* expression level in the ZD1839-treated *Gan* mice was still at the high level compared with WT mice. These results collectively indicate that EGFR activation is required for gastric tumorigenesis, even if the Wnt and $PGE_2$ pathways are activated.

**Suppression of tumor cell proliferation by EGFR inhibition.** Two major pathways downstream of EGFR signaling are the MAPK and PI3K/Akt pathways.[32] The levels of phosphorylated Akt and Erk1/2 were significantly decreased by ZD1839 treatment in the *Gan* mouse gastric tumors (Fig. 5a,b). Notably, celecoxib treatment also suppressed the phosphorylation of Akt and Erk1/2 to a similar level as in the ZD1839-treated mice, suggesting that induction of $PGE_2$ pathway is a major mechanism for activation of EGFR in gastric tumors.

Most tumor cells were immunostained for Ki-67 in the control *Gan* mice, while the number of Ki-67 positive cells was significantly decreased both in the ZD1839-treated and celecoxib-treated mice (Fig. 5c,d). Accordingly, it is possible that the $PGE_2$ pathway accelerates tumor cell proliferation through EGFR activation.

## Discussion

We found that there was simultaneous gene upregulation of EGFR ligands, *Areg*, *Ereg*, *Hbegf* and *Btc*, in the mouse gastric tumors, which occurred in a $PGE_2$-dependent manner. $PGE_2$



doi: 10.1111/j.1349-7006.2011.01847.x

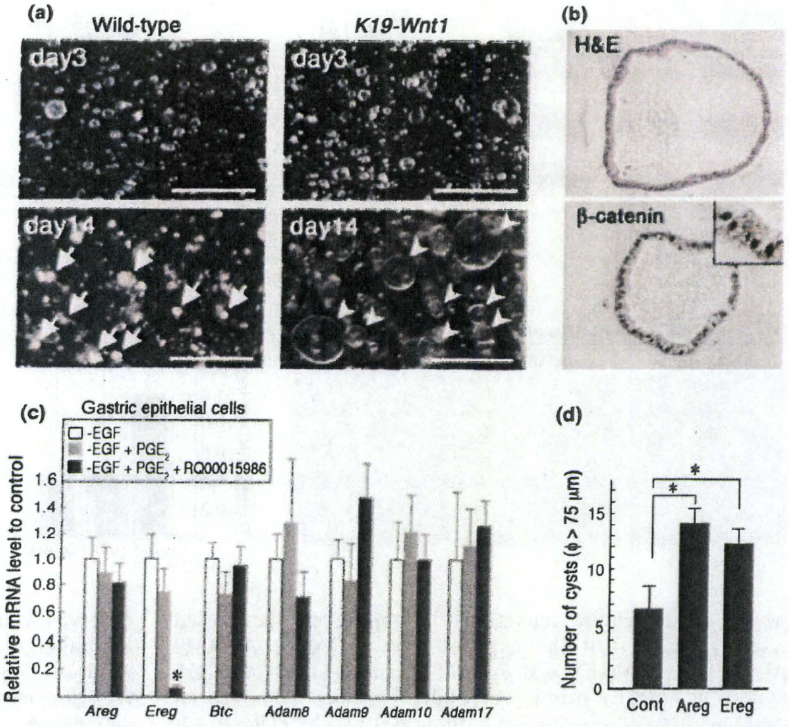


**Fig. 3.** (a) Representative photographs of the primary cultured gastric epithelial cells in matrigel from wild type (*left*) and *K19-Wnt1* mice (*right*). Arrowheads indicate cystic structures, while arrows indicate clusters of dead cells. Bars indicate 500 μm. (b) Histology (top, H&E) and immunostaining with anti-active β-catenin antibody (bottom) of cystic structures. Inset indicates nuclear accumulation of active β-catenin in the epithelial cells. (c) Relative expression of epidermal growth factor receptor (EGFR) ligands and a disintegrin and metalloproteinases (ADAMs) in gastric epithelial cells cultured in matrigel with the indicated treatment (mean ± SD). Asterisk indicates $P < 0.05$ versus the level in control cells cultured in EGF (−) medium. (d) The mean number of cystic structures >75 μm in diameter in matrigel of the amphiregulin-treated (*Areg*), epiregulin-treated (*Ereg*) and control (*cont*) gastric epithelial cells (mean ± SD). Asterisks indicate $P < 0.05$.

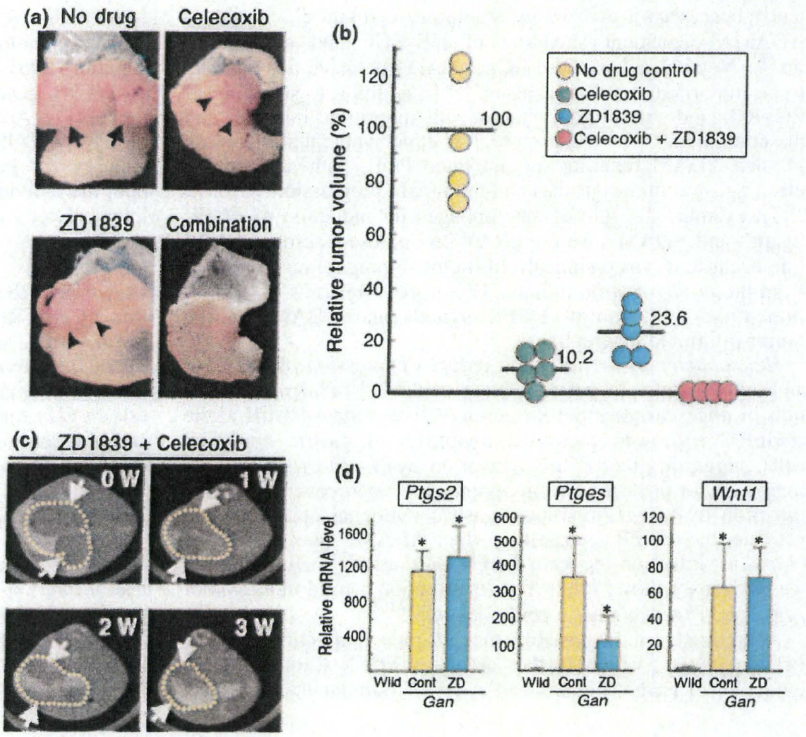


**Fig. 4.** (a) Representative photographs of *Gan* mouse stomach; no-drug control (top left), celecoxib-treated (top right), ZD1839-treated (bottom left), and treated with a combination of ZD1839 and celecoxib (bottom right). Arrows indicate gastric tumors in control mouse, whereas arrowheads indicate regressed tumors in the drug-treated mice. (b) Tumor volumes of *Gan* mice treated with celecoxib, ZD1839, and a combination of ZD1839 and celecoxib relative to control mice. Each filled circle indicates the value of individual mice, and the means of the respective groups are indicated. (c) X-ray computed tomography images of the same *Gan* mouse treated with a combination of ZD1839 and celecoxib at weeks 0, 1, 2 and 3 after starting drug administration. Yellow dashed lines indicate the stomach. Arrows indicate gastric tumors. (d) The mRNA levels of *Ptgs2*, *Ptges*, and *Wnt1* examined by real-time RT-PCR in the gastric tumors of no-drug control (Cont) and ZD1839-treated (ZD) *Gan* mice relative to wild-type level (wild) (mean ± SD). Asterisks indicate $P < 0.05$ versus wild-type level.

signaling through the EP4 receptor is required for basal expression of *Ereg* in epithelial cells, whereas both *Areg* and *Ereg* are induced by EP4 signaling in macrophages. On the other hand, *Hbegf* is induced in the activated macrophages in a $PGE_2$-independent manner. Accordingly, it is possible that expression of the respective EGFR ligands is regulated not only by $PGE_2$ signaling but also by $PGE_2$-induced inflammation in the different cell types including macrophages and epithelial cells.

It has been reported that $PGE_2$ signaling activates MMPs and ADAM17, resulting in shedding of TGF-α or amphiregulin,

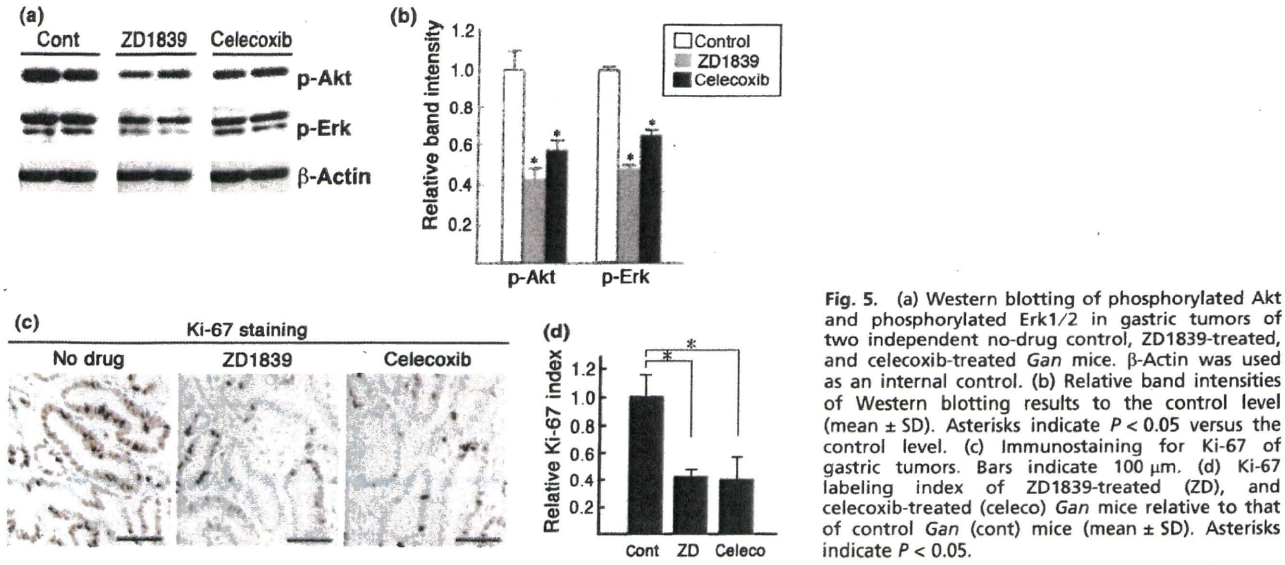


**Fig. 5.** (a) Western blotting of phosphorylated Akt and phosphorylated Erk1/2 in gastric tumors of two independent no-drug control, ZD1839-treated, and celecoxib-treated *Gan* mice. β-Actin was used as an internal control. (b) Relative band intensities of Western blotting results to the control level (mean ± SD). Asterisks indicate $P < 0.05$ versus the control level. (c) Immunostaining for Ki-67 of gastric tumors. Bars indicate 100 μm. (d) Ki-67 labeling index of ZD1839-treated (ZD), and celecoxib-treated (celeco) *Gan* mice relative to that of control *Gan* (cont) mice (mean ± SD). Asterisks indicate $P < 0.05$.

which causes EGFR activation.[12,15] However, the present results indicate that the expression of ADAM8, ADAM9, ADAM10, ADAM17, and ADAM28 are induced in gastric tumors in a $PGE_2$ pathway-dependent manner. Although we could not find direct induction of these ADAMs by $PGE_2$ in epithelial cells or macrophages, it is possible that $PGE_2$-associated inflammation induces these ADAMs indirectly. It has consistently been shown that the inflammatory cytokine IL-8 induces ADAM10-dependent shedding of HB-EGF and amphiregulin.[33] Notably, all of these induced ADAMs have been shown to be important in tumorigenesis.[27] In addition to shedding of EGFR ligands, they induce tumor cell migration, invasion and dissemination.[27,34,35] Therefore, it is conceivable that induction of such ADAM functions by activated $PGE_2$ pathway contributes to gastric tumorigenesis and malignant progression.

To examine the role of macrophages for induction of EGFR ligands and ADAMs, we used RAW264 mouse macrophage cell line because it was technically difficult to prepare macrophages from the *in vivo* gastric tumors. Therefore, it remains to be confirmed the induction of EGFR ligands and ADAMs in the tumor-infiltrated macrophages.

*Helicobacter pylori* infection induces expression of HB-EGF and amphiregulin in gastric cancer cells.[36–38] *H. pylori* infection in mice carrying the kinase-defective mutant EGFR allele ($EGFR^{wa2}$) showed increased apoptosis of gastric epithelial cells, suggesting that EGFR activation by *H. pylori* infection is important for protection from apoptosis.[39] Moreover, *H. pylori* infection to *Adam17*-disrupted gastric epithelial cells failed to activate the EGFR, suggesting that ADAMs play a role in *H. pylori* infection-induced EGFR activation.[39] Importantly, we previously showed that *H. felis* infection caused induction of *Ptgs2* and *Ptges* in gastric epithelial cells.[16]

Accordingly, it is possible that *H. pylori* infection induces $PGE_2$ pathway, which further activates EGFR through global induction of EGFR ligands and ADAMs, similar to the effects observed in the *C2mE* group mice. It is therefore possible that inhibition of the $PGE_2$ pathway, as well as eradication of *H. pylori* infection, can suppress EGFR activation in the *H. pylori*-infected gastric mucosa, thereby preventing gastric carcinogenesis.

The level of $PGE_2$ is regulated by 15-hydroxyprostaglandin dehydrogenase (15-PGDH), which inactivates prostaglandins. Importantly, expression of 15-PGDH is downregulated by EGFR signaling in colon cancer cells,[40] indicating that EGFR signaling activates $PGE_2$ pathway. Moreover, disruption of the 15-PGDH gene accelerates intestinal tumorigenesis in mouse models.[41] Accordingly, it is possible that inhibition of both $PGE_2$ and EGFR pathways represents an effective therapeutic strategy for gastrointestinal tumorigenesis by suppression of both the individual signaling pathways and the positive feedback loop between two signaling pathways. Among the four $PGE_2$ receptors, EP4 is the most abundant receptor in mouse gastric tumor models[24] and in human colon cancer tissues.[42] We have shown here that EP4 signaling is responsible for global induction of EGFR ligands and ADAMs through direct or indirect mechanisms, and macrophages are major source of EGFR ligands. Moreover, we have recently demonstrated that inhibition of EP4 signaling significantly suppressed gastric tumorigenesis in *Gan* mice.[43] These results, taken together, suggest that combination treatment with inhibitors of EGFR and EP4 will be an effective strategy for preventing gastric tumorigenesis.

## Acknowledgments

We wish to thank M. Watanabe for excellent technical assistance, and H. Itadani and H. Kotani for microarray analyses. This study was supported by Grants-in-Aid for the Third-Term Comprehensive Cancer Control Strategy from the Ministry of Health, Labor, and Welfare, Grant-in-Aids from the Ministry of Education, Science, Culture, and Sports of Japan, and Takeda Science Foundation.

## References

1 Gupta RA, DuBois RN. Colorectal cancer prevention and treatment by inhibition of cyclooxygenase-2. *Nat Rev Cancer* 2001; 1: 11–21.
2 Wang D, DuBois RN. Eicosanoids and cancer. *Nat Rev Cancer* 2010; **10**: 181–93.
3 Oshima M, Dinchuk JE, Kargman SL *et al.* Suppression of intestinal polyposis in $Apc^{\Delta 716}$ knockout mice by inhibition of cyclooxygenase 2 (COX-2). *Cell* 1996; **87**: 803–9.
4 Sonoshita M, Takaku K, Sasaki N *et al.* Acceleration of intestinal polyposis through prostaglandin receptor $EP_2$ in $Apc^{\Delta 716}$ knockout mice. *Nat Med* 2001; **7**: 1048–51.



doi: 10.1111/j.1349-7006.2011.01847.x

5 Seno H, Oshima M, Ishikawa T *et al.* Cyclooxygenase 2- and prostaglandin $E_2$ receptor $EP_2$-dependent angiogenesis in *Apc*$^{\Delta 716}$ mouse intestinal polyps. *Cancer Res* 2002; **62**: 506–11.
6 Dannenberg AJ, Lippman SM, Mann JR, Subbaramaiah K, DuBois RN. Cyclooxigenase-2 and epidermal growth factor receptor: pharmacologic targets for chemoprevention. *J Clin Oncol* 2005; **2**: 254–66.
7 Roberts RB, Min L, Washington MK *et al.* Importance of epidermal growth factor receptor signaling in establishment of adenomas and maintenance of carcinomas during intestinal tumorigenesis. *Proc Natl Acad Sci USA* 2002; **99**: 1521–6.
8 Torrance CJ, Jackson PE, Montgomery E *et al.* Combinatorial chemoprevention of intestinal neoplasia. *Nat Med* 2006; **6**: 1024–8.
9 Buchanan FG, Holla V, Katkuri S, Matta P, DuBois RN. Targeting cyclooxygenase-2 and the epidermal growth factor receptor for the prevention and treatment of intestinal cancer. *Cancer Res* 2008; **67**: 9380–8.
10 Buchanan FG, Wang D, Bargiacchi F, DuBois RN. Prostaglandin $E_2$ regulates cell migration via the intracellular activation of the epidermal growth factor receptor. *J Biol Chem* 2003; **278**: 35451–7.
11 Buchanan FG, Gorden DL, Matta P, Shi Q, Matrisian LM, DuBois RN. Role of β-arrestin1 in the metastatic progression of colorectal cancer. *Proc Natl Acad Sci USA* 2006; **103**: 1492–7.
12 Pai R, Soreghan B, Szabo IL, Pavelka M, Baatar D, Tarnawski AS. Prostaglandin $E_2$ transactivates EGF receptor: a novel mechanism for promoting colon cancer growth and gastrointestinal hypertrophy. *Nat Med* 2002; **8**: 289–93.
13 Shao J, Lee SB, Guo H, Evers BM, Sheng H. Prostaglandin $E_2$ stimulates the growth of colon cancer cells via induction of amphiregulin. *Cancer Res* 2003; **63**: 5218–23.
14 Subbaramaiah K, Benezra R, Hudis C, Dannenberg AJ. Cyclooxygenase-2-derived prostaglandin $E_2$ stimulates *Id-1* transcription. *J Biol Chem* 2008; **283**: 33955–68.
15 Al-Salihi MA, Ulmer SC, Doan T *et al.* Cyclooxygenase-2 transactivates the epidermal growth factor receptor through specific E-prostanoid receptors and tumor necrosis factor-α converting enzyme. *Cell Signal* 2007; **19**: 1956–63.
16 Oshima H, Oshima M, Inaba K, Taketo MM. Hyperplastic gastric tumors induced by activated macrophages in COX-2/mPGES-1 transgenic mice. *EMBO J* 2004; **23**: 1669–78.
17 Guo X, Oshima H, Kitamura T, Taketo MM, Oshima M. Stromal fibroblasts activated by tumor cells promote angiogenesis in mouse gastric cancer. *J Biol Chem* 2008; **283**: 19864–71.
18 Stadtlander CT, Waterbor JW. Molecular epidemiology, pathogenesis and prevention of gastric cancer. *Carcinogenesis* 1999; **20**: 2195–207.
19 Saukkonen K, Rintahaka J, Sivula A *et al.* Cyclooxygenase-2 and gastric carcinogenesis. *APMIS* 2003; **111**: 915–25.
20 Thun MJ, Namboodiri MM, Calle EE, Flanders WD, Heath CW Jr. Aspirin use and risk of fatal cancer. *Cancer Res* 1993; **53**: 1322–7.
21 Clements WM, Wang J, Sarnaik A *et al.* *β-Catenin* mutation is a frequent cause of Wnt pathway activation in gastric cancer. *Cancer Res* 2002; **62**: 3503–6.
22 Oshima H, Matsunaga A, Fujimura T, Tsukamoto T, Taketo MM, Oshima M. Carcinogenesis in mouse stomach by simultaneous activation of the Wnt signaling and prostaglandin $E_2$ pathway. *Gastroenterology* 2006; **131**: 1086–95.
23 Itadani H, Oshima H, Oshima M, Kotani H. Mouse gastric tumor models with prostaglandin $E_2$ pathway activation show similar gene expression profiles to intestinal-type human gastric cancer. *BMC Genomics* 2009; **10**: 615.
24 Oshima H, Itadani H, Kotani H, Taketo MM, Oshima M. Induction of prostaglandin $E_2$ pathway promotes gastric hamartoma development with suppression of bone morphogenetic protein signaling. *Cancer Res* 2009; **69**: 2729–33.
25 Oshima H, Oguma K, Du YC, Oshima M. Prostaglandin $E_2$, Wnt and BMP in gastric tumor mouse models. *Cancer Sci* 2009; **100**: 1779–85.
26 Takeuchi K, Tanaka A, Kato S, Aihara E, Amagase K. Effect of (*S*)-4-(1-(5-Chloro-2-(4-fluorophenyoxy)benzamido)ethyl) benzoic acid (CJ-42794), a selective antagonist of prostaglandin E receptor subtype 4, on ulcerogenic and healing responses in rat gastrointestinal mucosa. *J Pharmacol Exp Ther* 2007; **322**: 903–12.
27 Mochizuki S, Okada Y. ADAMs in cancer cell proliferation and progression. *Cancer Sci* 2007; **98**: 621–8.
28 Sahin U, Weskamp G, Kelly K *et al.* Distinct roles for ADAM10 and ADAM17 in ectodomain shedding of six EGFR ligands. *J Cell Biol* 2004; **164**: 769–79.
29 Sanderson MP, Erickson SN, Gough PJ *et al.* ADAM10 mediates ectodomain shedding of the betacellulin precursor activated by *p*-aminophenylmercuric acetate and extracellular calcium influx. *J Biol Chem* 2005; **280**: 1826–37.
30 Horiuchi K, Gall SL, Schulte M *et al.* Substrate selectivity of epidermal growth factor-receptor ligand sheddases and their regulation by phorbol esters and calcium influx. *Mol Biol Cell* 2007; **18**: 176–88.
31 Pollard JW. Trophic macrophages in development and disease. *Nat Rev Immunol* 2009; **9**: 259–70.
32 Yarden Y, Sliwkowski MX. Untangling the ErbB signaling network. *Nat Rev Mol Cell Biol* 2001; **2**: 127–37.
33 Tanida S, Joh T, Itoh K *et al.* The mechanism of cleavage of EGFR ligands induced by inflammatory cytokines in gastric cancer cells. *Gastroenterology* 2004; **127**: 559–69.
34 Mazzocca A, Coppari R, De Franco R *et al.* A secreted form of ADAM9 promotes carcinoma invasion through tumor-stromal interactions. *Cancer Res* 2005; **65**: 4728–38.
35 Fogel M, Gutwein P, Mechtersheimer S *et al.* L1 expression as a predictor of progression and survival in patients with uterine and ovarian carcinomas. *Lancet* 2003; **362**: 869–75.
36 Romano M, Ricci V, Di Popolo A *et al.* *Helicobacter pylori* upregulates expression of epidermal growth factor-related peptides, but inhibits their proliferative effect in MKN28 gastric mucosal cells. *J Clin Invest* 1998; **101**: 1604–13.
37 Keates S, Sougioultzis S, Keates AC *et al.* cag+ *Helicobacter pylori* induce transactivation of the epidermal growth factor receptor in AGS gastric epithelial cells. *J Biol Chem* 2001; **276**: 48127–34.
38 Wallasch C, Crabtree JE, Bevec D *et al.* *Helicobacter pylori*-stimulated EGF receptor transactivation requires metalloprotease cleavage of HB-EGF. *Biochem Biophys Res Commun* 2002; **295**: 695–710.
39 Yan F, Cao H, Chaturvedi R *et al.* Epidermal growth factor receptor activation protects gastric epithelial cells from *Helicobacter pylori*-induced apoptosis. *Gastroenterology* 2009; **136**: 1297–307.
40 Mann JR, Backlund MG, Buchanan FG *et al.* Repression of prostaglandin dehydrogenase by epidermal growth factor and snail increases prostaglandin $E_2$ and promotes cancer progression. *Cancer Res* 2006; **66**: 6649–56.
41 Myung SJ, Rerko RM, Yan M *et al.* 15-hydroxyprostaglandin dehydrogenase is an in vivo suppressor of colon tumorigenesis. *Proc Natl Acad Sci USA* 2006; **103**: 12098–102.
42 Doherty GA, Byrne SM, Molloy ES *et al.* Proneoplastic effects of $PGE_2$ mediated by EP4 receptor in colorectal cancer. *BMC Cancer* 2009; **9**: 207.
43 Oshima H, Hioki K, Popivanova BK *et al.* Prostaglandin E2 signaling and bacterial infection recruit tumor-promoting macrophages to mouse gastric tumors. *Gastroenterology* 2010 Nov 9. [Epub ahead of print]

THE JOURNAL OF BIOLOGICAL CHEMISTRY VOL. 285, NO. 24, pp. 18283–18290, June 11, 2010


# LKB1 Suppresses p21-activated Kinase-1 (PAK1) by Phosphorylation of Thr$^{109}$ in the p21-binding Domain*[S]

Received for publication, October 25, 2009, and in revised form, March 22, 2010 Published, JBC Papers in Press, April 16, 2010, DOI 10.1074/jbc.M109.079137

**Atsuko Deguchi[‡], Hiroyuki Miyoshi[‡], Yasushi Kojima[‡], Katsuya Okawa[§], Masahiro Aoki[‡], and Makoto M. Taketo[‡1]**

*From the [‡]Department of Pharmacology, Graduate School of Medicine, Kyoto University, Kyoto 606-8501, Japan and [§]Drug Discovery Research Laboratories, Kyowa Hakko Kirin Co., Ltd., Shizuoka 411-8731, Japan*

**The serine/threonine protein kinase *LKB1* is a tumor suppressor gene mutated in Peutz-Jeghers syndrome patients. The mutations are found also in several types of sporadic cancer. Although LKB1 is implicated in suppression of cell growth and metastasis, the detailed mechanisms have not yet been elucidated. In this study, we investigated the effect of LKB1 on cell motility, whose acquisition occurs in early metastasis. The knockdown of LKB1 enhanced cell migration and PAK1 activity in human colon cancer HCT116 cells, whereas forced expression of LKB1 in *Lkb1*-null mouse embryonic fibroblasts suppressed PAK1 activity and PAK1-mediated cell migration simultaneously. Notably, LKB1 directly phosphorylated PAK1 at Thr$^{109}$ in the p21-binding domain *in vitro*. The phosphomimetic T109E mutant showed significantly lower protein kinase activity than wild-type PAK1, suggesting that the phosphorylation at Thr$^{109}$ by LKB1 was responsible for suppression of PAK1. Consistently, the nonphosphorylatable T109A mutant was resistant to suppression by LKB1. Furthermore, we found that PAK1 was activated in the hepatocellular carcinomas and the precancerous liver lesions of *Lkb1*(+/−) mice. Taken together, these results suggest that PAK1 is a direct downstream target of LKB1 and plays an essential role in LKB1-induced suppression of cell migration.**

LKB1 is a serine/threonine kinase whose mutations have been found not only in Peutz-Jeghers syndrome patients (1–3) but also in various types of sporadic cancer (4–6). These results suggest that *LKB1* is a tumor suppressor gene. In addition, we and others (7–9) have previously shown that the heterozygous *Lkb1* mutations in mice cause gastrointestinal hamartomas after 20 weeks of age and cause hepatocellular carcinomas (HCCs)[2] after 50 weeks (10). Notably, the *Lkb1* gene in all HCC and hepatic precancerous lesions shows loss of heterozygosity (10, 11). These phenotypes in *Lkb1*(+/−) mice further indicate that *LKB1* is a tumor suppressor gene.

In mammalian cells, LKB1 forms a complex with STE20-related adaptor pseudokinase (STRAD) and scaffolding protein MO25, both of which are required for LKB1 enzymatic activity (12, 13). It can phosphorylate and activate at least 14 kinases, including AMP-activated protein kinase (AMPK) and microtubule-associated protein/microtubule affinity-regulating kinases (MARKs) (5). Activation of AMPK by LKB1 leads to inactivation of mammalian target of rapamycin complex 1 via phosphorylation of the tuberous sclerosis complex 1/2, and this pathway has been implicated in tumor suppressor functions of LKB1. In addition to growth control, LKB1 also plays important roles in establishing cell polarity in mammalian cells (14). LKB1 regulates tight junction assembly and cell polarity through AMPK in mammalian cells (15, 16), and we have shown that LKB1 suppresses tubulin polymerization by activating MARK microtubule-associated protein signaling (17). We have also reported that HCCs in *Lkb1*(+/−) mice metastasize to the lungs (10). However, the mechanisms by which LKB1 suppresses cancer metastasis have not yet been explored. In this study, we have investigated the effect of LKB1 on cell motility whose acquisition occurs in early metastasis (18).

The serine/threonine kinase PAK1 is known as a key regulator of cell motility, proliferation, differentiation, and survival (19). It can activate diverse signaling pathways, including LIM motif-containing protein kinase 1, mitogen-activated protein kinase (MAPK), and NF-κB signaling (20). PAK1 interacts with the GTP-bound forms of Cdc42 or Rac, which cause PAK1 activation (21). In addition to activation by Cdc42/Rac, its activity is positively regulated also by other signaling molecules, including phosphoinositide 3-kinase (22), 3-phosphoinositide-dependent kinase-1 (23), and AKT (24).

PAK1 is overexpressed in various types of cancer, including breast (25, 26), colon (27), and liver (28) cancers. A high level of PAK1 expression is correlated with more aggressive tumor behaviors such as metastatic phenotype and advanced tumor stages in hepatocellular carcinomas (28) as well as in colorectal cancer (27). Consistently, overexpression of constitutively active mutant PAK1 (T423E) helps develop malignant mammary tumors in a transgenic mouse model (29). These results indicate that PAK1 plays a key role in carcinogenesis and cancer metastasis. Here, we present evidence that LKB1 inhibits cell motility and PAK1-mediated signaling through direct phosphorylation of PAK1 at Thr$^{109}$ in the p21-binding domain.

* This work was supported by a grant-in-aid for scientific research (to M. M. T.), a grant-in-aid for young scientist (B) from the Ministry of Education, Culture, Sports, Science and Technology of Japan, and Littlefield-American Association for Cancer Research grants in metastatic colon cancer research (to M. M. T.).

[S] The on-line version of this article (available at http://www.jbc.org) contains supplemental "Experimental Procedures" and Fig. S1.

[1] To whom correspondence should be addressed: Dept. of Pharmacology, Graduate School of Medicine, Kyoto University, Yoshida-Konoé-cho, Sakyo-ku, Kyoto 605-8501, Japan. Tel.: 81-75-753-4391; Fax: 81-75-753-4402; E-mail: taketo@mfour.med.kyoto-u.ac.jp.

[2] The abbreviations used are: HCC, hepatocellular carcinoma; PAK1, p21-activated kinase-1; PBD, p21-binding domain; Adv, adenovirus; AMPK, AMP-activated protein kinase; STRAD, STE20-related adaptor pseudo-kinase; MARK, microtubule-associated protein/microtubule affinity-regulating kinase; siRNA, small interfering RNA; wt, wild-type; GST, glutathione *S*-transferase; HA, hemagglutinin; VASP, vasodilator-stimulated phosphoprotein.

## EXPERIMENTAL PROCEDURES

*Cell Culture*—HCT116 cells and HEK293T cells were maintained in low glucose Dulbecco's modified Eagle's medium (Nacalai Tesque, Kyoto, Japan) supplemented with 10% fetal bovine serum (BioWest, Nuaillé, France), and 100 units of penicillin/streptomycin.

*Mice*—Construction of *Lkb1* knock-out mice has been described previously (10). We only used males due to the low incidence of nodular foci and HCCs in female *Lkb1*(+/−) mice, as reported previously. All animal experiments were approved by the Animal Care and Use Committee of Kyoto University.

*Reagents*—A mouse monoclonal anti-LKB1 (clone Ley37D/G6), anti-Myc (clone 9E10) and rabbit polyclonal anti-PAK1 antibodies were purchased from Santa Cruz Biotechnology (Santa Cruz, CA). Rabbit polyclonal anti-phospho-PAK1 ($Ser^{144}$)/PAK2 ($Ser^{141}$), anti-phospho-PAK1 ($Ser^{199/204}$)/PAK2 ($Ser^{201}$), anti-PAK1 and anti-phospho-Vasodilator-stimulated phosphoprotein (VASP) ($Ser^{239}$) antibodies were from Cell Signaling Technology (Danvers, MA), and rabbit polyclonal anti-VASP antibody was from EMD Chemicals (Gibbstown, NJ). A mouse monoclonal anti-β-actin antibody was from Sigma-Aldrich (St. Louis, MO), and a mouse monoclonal anti-Hemagglutinin antibody was from Invivogen (San Diego, CA). Two different small interfering RNAs against human LKB1, and scramble siRNA pools were purchased from Dharmacon, Inc. (Lafayette, CO).

*cDNA*—The following cDNAs were isolated by standard PCR-based cloning techniques: human LKB1, NCBI accession no. NM_000455 and human STRAD, respectively, NCBI accession no. NM_001003787. HA and FLAG tags were attached to the N termini of LKB1 and STRAD, as described previously (17). LKB1 (kinase-dead, a catalytically inactive version of LKB1 with a D194A mutation (30)), was generated with QuikChange II site-directed mutagenesis kit (Stratagene, La Jolla, CA) according to the manufacturer's protocol. Wild-type of PAK1, constitutively active mutant T423E, and a dominant-negative mutant H83LH86LK299R were kindly gifted by Dr. Jonathan Chernoff (Fox Chase Cancer Center). Appropriate PCR primers were used to generate the point mutants PAK1-T109E and PAK1-T109A with the QuikChange II site-directed mutagenesis kit. These BamHI/EcoRI fragments were subcloned into pCMV-Tag 3B (Stratagene), which has an N-terminal Myc tag and a cytomegalovirus promoter.

*PAK1-K299R Lentivirus*—The NotI/SalI fragment of pCMV-Tag3B-PAK1-K299R was subcloned into pLEX vector (Open Biosystems, Huntsville, AL). Recombinant lentivirus encoding K299R was prepared according to the manufacturer's protocol.

*Establishment of an Lkb1-null Mouse Embryonic Fibroblast (MEF) Cell Line*—*Lkb1*(+/−) mice (C57BL/6N background) were crossed with outbred ICR mice, and offspring were intercrossed. *Lkb1*-null embryos at 9.5 days post-coitum were minced, trypsinized briefly, and placed on 24-well plates. These cells were cultured in RPMI 1640 (Sigma) with 10% (v/v) fetal bovine serum and 50% (v/v) conditioned medium from the MEFs that were derived from wild-type embryos at 12.5 days post-coitum. We obtained a spontaneously immortalized cell line (MEF3) by continuous passages (>3 months) of the *Lkb1*-null MEFs and further established the subclone MEF3-2 cell line. Finally, we cultured MEF3-2 in Dulbecco's modified Eagle's medium (Sigma) with 10% (v/v) fetal bovine serum.

*Recombinant Adenoviruses*—Recombinant adenoviruses were constructed by Adeno-X expression system 1 (Clontech Laboratories, Mountain View, CA), according to the manufacturer's protocol. The titers of the recombinant adenoviruses were determined by the method previously reported by others (31).

*Wound-healing Assay*—Cells were infected with recombinant adenovirus; after 24 h of infection, wounds were incised by scratching the cell monolayer using 10-μl pipette tips. Photographs were taken at 0 and 20 h after the wound was made. Cell migration was normalized so that 100% represents the migration distance of control cells.

*Transfection*—HEK293T cells were transfected with plasmid DNA of the indicated PAK1 and LKB1 expression vectors using Lipofectamine 2000 (Invitrogen). After 24 h of transfection, cell lysates were prepared for Western blotting or *in vitro* kinase assay. Lipofectamine 2000 RNAiMAX (Invitrogen) was used for small interfering RNA (siRNA) transfection according to manufacturer's protocol.

*Recombinant PAK1 Proteins Produced in Escherichia coli*—PAK1-PBD was isolated by standard PCR-based cloning techniques. The PAK1-PBD-T109A mutant was generated with the QuikChange II site-directed mutagenesis kit. To attach GST protein to PAK1-PBD, PAK1-PBD-T109A, PAK1-K299R, or PAK1-T109A/K299R was inserted in the BamHI-double digested pGEX-6P-1 vector (GE Healthcare). pGEX-2TK-VASP-(158–277) was generated previously (32). 200 ml of 2×YT medium (1.6% tryptone, 1% yeast extract, and 0.5% NaCl) medium was inoculated with *E. coli* (BL21 strain) containing the recombinant pGEX-2TK plasmid that encodes GST-VASP-(158–277), or the recombinant pGEX-6P-1 plasmid that encodes GST-PAK1-PBD, GST-PAK1-PBD-T109A, GST-PAK1-K299R, or GST-PAK1-T109A/K299R and was incubated at 37 °C in the presence of 100 μg/ml ampicillin until $A_{600}$ reached 0.8. To induce expression of the GST-tagged proteins, isopropyl-D-thiogalactopyranoside was added at 100 μM. After culture for 24 additional hours at 25 °C, cells were harvested, and recombinant proteins were purified as described previously (17).

*Western Blotting*—Cells were lysed in the lysis buffer (50 mM Tris-HCl (pH 7.4), 150 mM NaCl, 5 mM $Na_4P_2O_7$, 10 mM β-glycerophosphate, 25 mM NaF, 1 mM EDTA, 1 mM EGTA, 1 mM $Na_3VO_4$, and 1% (v/v) Triton X-100) containing Complete mini protease inhibitor mixture (Roche Applied Science). Cell lysates were separated by SDS-PAGE and transferred to Immobilon-P membrane (Millipore, Billerica, MA). After blocking with Blocking One or Blocking One-P (Nacalai Tesque, Kyoto, Japan), the membranes were probed with the indicated antibodies. The signals were visualized by Immobilon western detection system (Millipore) or ECL Western blotting detection reagents (GE Healthcare).

*In Vitro Phosphorylation Assay*—Phosphorylation reactions were performed at 30 °C in the phosphorylation reaction buffer (50 mM Tris-HCl (pH 7.0), 10 mM $MgCl_2$, 2 mM $MnCl_2$, 5 mM β-glycerophosphate, 100 μM $Na_3VO_4$, 1 mM dithiothreitol, and

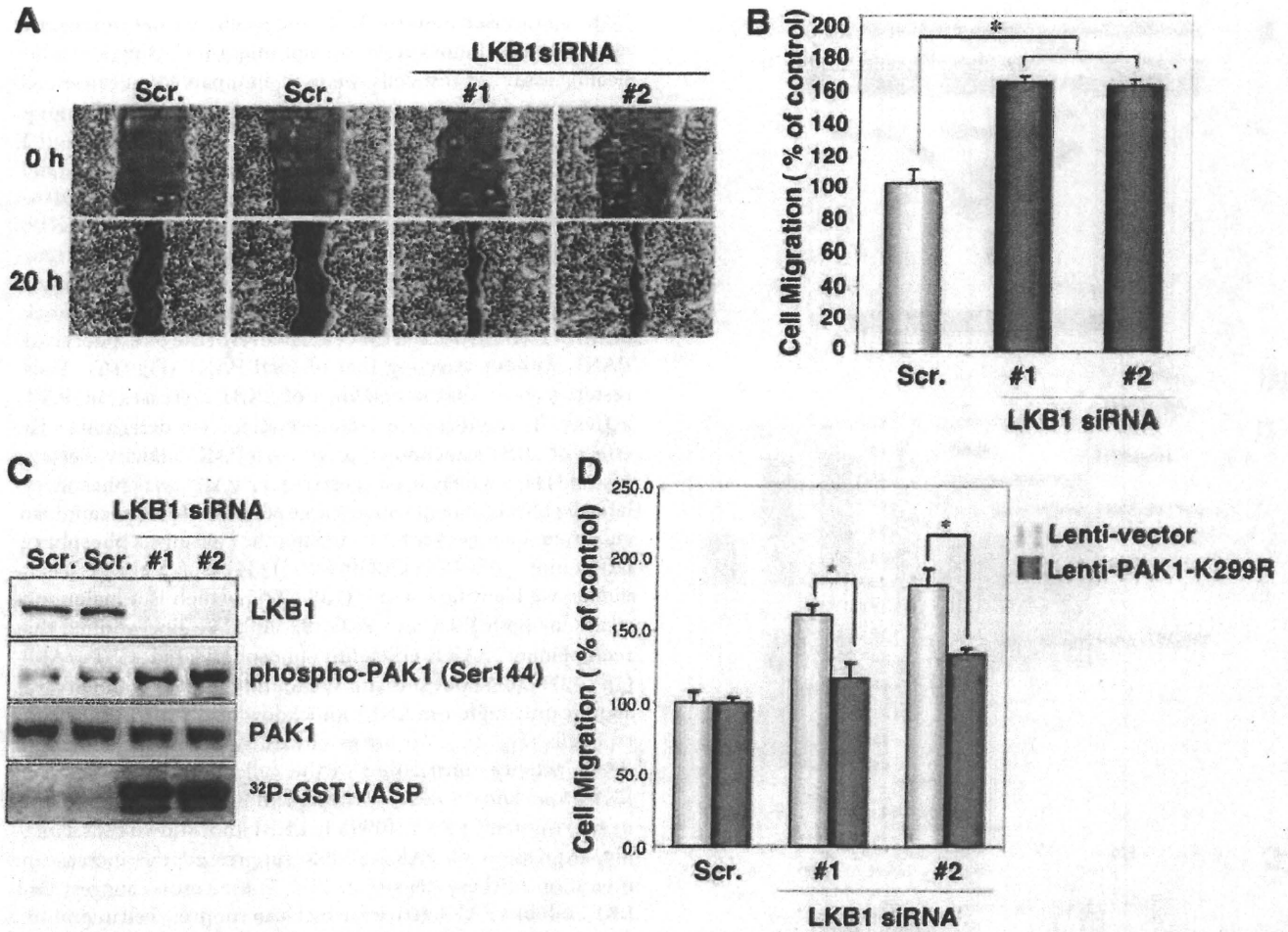


FIGURE 1. **Knockdown of endogenous LKB1 increases cell migration and PAK1 activity in HCT116 cells.** *A*, knockdown of LKB1 increases cell migration. HCT116 cells were transfected with two different specific siRNAs against human LKB1. Control cells were transfected with a scrambled (*Scr.*) siRNA pool. After 24 h of plating, scratches were made with 10-$\mu$l pipette tips. Photographs were taken at 0 and 20 h after the wound was made. *B*, cell migration was normalized so that 100% represented migration distance of control cells. *Error bars* indicate S.D. The *asterisk* indicates significant increases compared with control cells ($p < 0.001$). *C*, cellular levels of phospho-PAK1 ($Ser^{144}$), total PAK1 and *in vitro* PAK1 activity in LKB1 knockdown HCT116 cells. Lysates were prepared from HCT116 cells transfected with the indicated siRNAs. The levels of phospho-PAK1 ($Ser^{144}$) and PAK1 were determined by Western blotting with the indicated antibodies. Lysates were prepared from HCT116 cells transfected with the indicated siRNAs and immunoprecipitated using an anti-PAK1 antibody. The precipitates were used for *in vitro* kinase assays using GST-VASP-(158–277) as a substrate. The phosphorylation of GST-VASP was visualized using BAS-5000 Bio-imaging Analyzer. *D*, induction of PAK1-K299R suppressed the increase in migration in LKB1 knockdown cells. The cells transfected with the indicated siRNAs were then infected with lentivirus lenti-PAK1-K299R or lenti-vector. At 24 h post-infection, cultures were scratches were made with 10-$\mu$l pipette tips. Photographs were taken at 0 and 20 h thereafter. Cell migration was normalized so that 100% represented the migration distance of control cells. *Error bars* indicate S.D. The *asterisk* represents significant increases compared with control cells ($p < 0.001$).

200 $\mu$M ATP). As shown in Figs. 1*C* and 2*B*, the immunoprecipitates obtained from cell lysates using anti-PAK1 antibody were incubated with GST-VASP-(158–277) for 20 min. The reactions were stopped by the addition of 3× sample buffer (150 mM Tris-HCl (pH 6.8), 6% (w/v) SDS, 0.03% (w/v) bromphenol blue, 30% (v/v) glycerol, and 15% (v/v) 2-mercaptoethanol). The anti-Myc immunoprecipitates from HEK293T cell lysates were incubated with 5 $\mu$g of GST-VASP-(158–277) for 20 min with [$\gamma$-$^{32}$P]-ATP (see Figs. 3*A* and 5). The reactions were then terminated by the addition of 3× sample buffer. The samples were electrophoresed on 5–20% SDS-PAGE gels. The blots were exposed to a phosphor imaging plate (Fujifilm, Tokyo, Japan). The signals were detected by using BAS-5000 Bio-imaging Analyzer (Fujifilm). All assays using [$\gamma$-$^{32}$P]ATP were done at the Radioisotope Research Center of Kyoto University. Fold induction was determined using NIH Image (version 1.62). Recombinant LKB1/STRAD/MO25 (Millipore) was preincubated with recombinant PAK1 (EMD Chemicals) in the presence of ATP for 20 min, and then the reaction mixtures were incubated with 5 $\mu$g of GST-VASP-(158–277) for 20 min (see Fig. 3*B*). The cellular levels of phosphorylated VASP were detected using an anti-phospho-VASP ($Ser^{239}$) antibody.

*Statistical Analysis*—Results of the experimental studies were reported as mean ± S.D. Differences were analyzed by Student's *t* test. A value of $p < 0.05$ was regarded as significant.

## RESULTS

*Knockdown of Endogenous LKB1 Enhances Cell Migration and PAK1 Activity in HCT116 Cells*—We have reported previously that HCCs in *Lkb1*(+/−) mice metastasize to the lungs (10). Consistently, LKB1 also appears to suppress lung cancer metastasis (33). To investigate the mechanism(s) by which

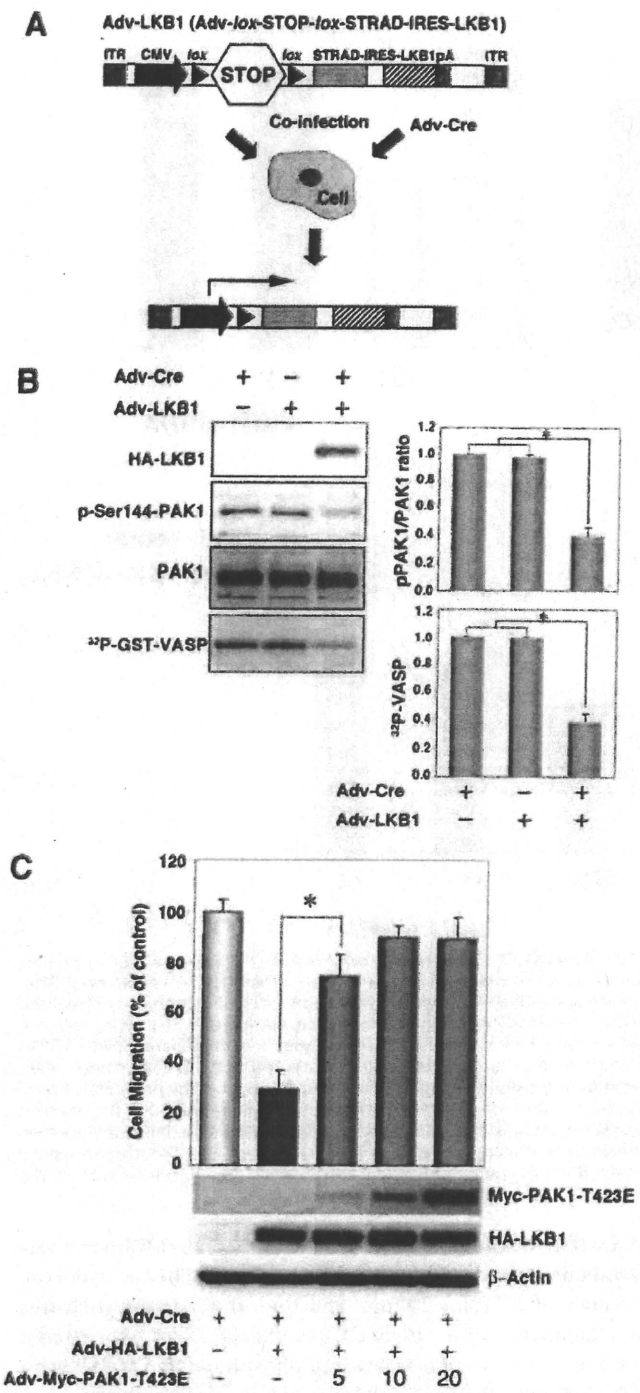


FIGURE 2. **Expression of LKB1 in the *Lkb1*-null MEF cell line (MEF3-2) inhibits cell migration and PAK1 activation.** *A*, schematic structure of the adenoviral construct, adapted from Ref. 17. *ITR*, inverted terminal repeat; *CMV*, human cytomegalovirus immediate early promoter; *lox*, loxP site sequence; *STOP*, transcriptional termination cassette; *IRES*, internal ribosome entry site; *pA*, polyadenylation signal. Co-infection with Adv-Cre removed the STOP cassette from Adv-LKB1. *B*, cellular levels of PAK1 autophosphorylation, total PAK1, and *in vitro* PAK1 activity in LKB1-expressing MEF3-2 cells. MEF 3-2 cells were co-infected with recombinant adenoviruses Adv-Cre and Adv-LKB1. Control cells were infected with Adv-Cre alone. The levels of phospho-PAK1 and PAK1 were determined by Western blotting with anti-phospho-PAK1 (Ser$^{144}$)/PAK2 (Ser$^{141}$) and anti-PAK1 antibodies, respectively. Lysates were prepared from MEF3-2 cells infected with the indicated recombinant adenoviruses and immunoprecipitated using an anti-PAK1 antibody. The precipitates were used for *in vitro* kinase assays with GST-VASP-(158–277) as a substrate. The phosphorylation of GST-VASP was visualized and quantified using BAS-5000 Bio-imaging Analyzer. *Error bars* indicate S.D. The *asterisk* represents significant decreases compared with control cells ($p < 0.001$). *C*, the constitutively active mutant of PAK1 rescues LKB1-induced suppression of cell migration in MEF3-2 cells. MEF 3-2 cells were co-infected with recombinant adenoviruses Adv-Cre, Adv-LKB1, and Adv-PAK1-T423E at a multiplicity of infection of 5, 10, or 20. Control cells were infected with Adv-Cre alone. Cell migration assays were performed as Fig. 1. *Error bars* indicate S.D. The *asterisk* represents significant changes in Adv-Cre/Adv-LKB1/Adv-PAK1-T423E (5) infected cells compared with Adv-Cre/Adv-LKB1-infected cells ($p < 0.001$). Similar results were obtained in three independent experiments.

LKB1 suppressed metastasis of cancer cells, we determined the effect of LKB1 knockdown on cell migration using a wound-healing assay. As test cells, we used a human colon cancer cell line HCT116 that expressed a significant level of LKB1 endogenously. HCT116 cells transfected with LKB1 siRNA (1 and 2) migrated 1.5× faster than those with scrambled siRNA pool (Fig. 1, *A* and *B*, *Scr.*). Because PAK1 is an important regulator of cell migration (34), we investigated a possible role of PAK1 in cell migration enhanced by LKB1 knockdown. To determine the PAK1 activity in LKB1 knockdown cells, we then analyzed the level of phospho-PAK1 (Ser$^{144}$), its active form (35). Knockdown of LKB1 increased the cellular level of the phosphorylated PAK1, without affecting that of total PAK1 (Fig. 1*C*). These results suggest that knockdown of LKB1 increases the PAK1 activity. To confirm this interpretation, we determined the effect of LKB1 knockdown on *in vitro* PAK1 activity. Because histone H4, a widely used substrate for PAK1, was phosphorylated by LKB1 (data not shown), we screened *in silico* candidate substrate sequences for PAK1 using the consensus phosphorylation motif ((K/R)(R/*X*)(*X*)(pS/pT)) (34) as a query. As a candidate, we identified VASP-(158–277), which is a major substrate for both PKA and PKG (32, 36). We first verified that recombinant PAK1 efficiently phosphorylated GST-VASP-(158–277) (data not shown). We found that PAK1 activity was significantly higher in LKB1 knockdown cells than in the control cells (Fig. 1*C*). To further investigate whether enhanced PAK1 activity contributed to the cell migration increase in LKB1 knockdown cells, we tested the effect of a dominant-negative mutant PAK1-K299R in LKB1 knockdown cells. Notably, expression of PAK1-K299R suppressed the increase in migration of these cells (Fig. 1*D*). These results suggest that LKB1 inhibits PAK1 activity, which can suppress cell migration.

*Expression of LKB1 in Lkb1-null MEFs Inhibits PAK1 Activity and Cell Migration*—To investigate the role of LKB1 in suppression of PAK1-mediated signaling, we further evaluated the effect of forced LKB1 expression on PAK1 activation in mouse embryonic fibroblasts that lack wild-type LKB1 (MEF3-2). To this end, we used the recombinant adenovirus encoding LKB1/STRAD (Adv-LKB1) that contained a transcription termination cassette (STOP sequence) flanked by the *loxP* sequences and expressed LKB1/STRAD by co-infection of MEF3-2 with Adv-Cre, which removed the STOP sequence from Adv-LKB1. The floxed inducible system was employed because LKB1 had some cytotoxic effects on host HEK293 cells and hampered production of the LKB1-expressing recombinant adenovirus. Such cytotoxicity was not observed with MEF3-2 cells up to 48 h post-induction. (Fig. 2*A*) (17). The cells infected with Adv-LKB1 alone showed

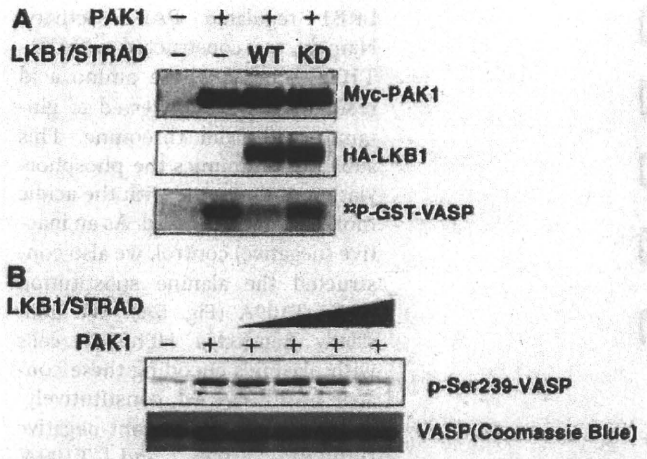


FIGURE 3. **LKB1 activity is necessary for suppression of PAK1 activity.** *A*, the wt LKB1, but not the kinase-dead mutant (*KD*), inhibits PAK1 activity. HEK293T cells were co-transfected with the indicated constructs. At 24 h post-transfection, immunoprecipitates were prepared with an anti-Myc antibody. The precipitates were used for *in vitro* kinase assays using GST-VASP-(158–277) as a substrate. The kinase activities were visualized using BAS-5000 Bio-imaging Analyzer. Cellular levels of Myc-PAK1 and HA-LKB1 were determined by Western blotting with anti-Myc or anti-HA antibody. *B*, recombinant LKB1 complex (LKB1-STRAD-MO25) directly inhibits PAK1 activity *in vitro* in a dose-dependent manner. The LKB1 complex (LKB1-STRAD-MO25) was preincubated with recombinant PAK1 and ATP in the absence of any PAK1 substrates, followed by addition of GST-VASP. The phosphorylated VASP was detected using an anti-phospho-VASP (Ser$^{239}$) antibody. Coomassie Brilliant Blue was used for detection of GST-VASP-(158–277). Similar results were obtained in three independent experiments.

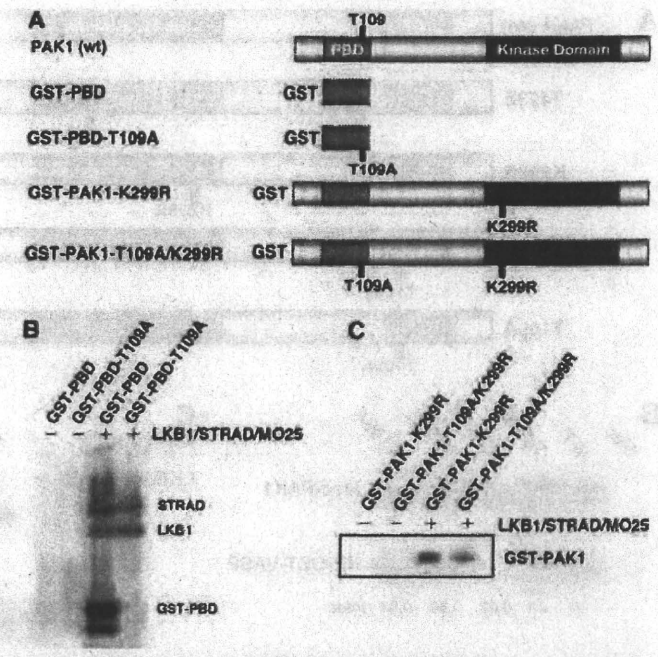


FIGURE 4. **LKB1 phosphorylates PAK1 *in vitro* at Thr$^{109}$.** *A*, schematic presentation of PAK1 and its mutant forms. wt PAK1 contains the p21-binding domain (*light gray*) and the kinase domain (*dark gray*). The noncatalytic domains are in *white*. Thr$^{109}$ is a possible phosphorylation site for LKB1. *B*, LKB1 phosphorylates GST-PAK1-PBD at Thr$^{109}$ *in vitro*. The recombinant LKB1 complex (LKB1-STRAD-MO25) was incubated with GST-PBD or GST-PBD-T109A. *C*, LKB1 phosphorylates full-length GST-PAK1-K299R and GST-PAK1-T109A/K299R to a lesser extent. The *in vitro* kinase assays were performed using the recombinant LKB1 complex with GST-PAK1-K299R or GST-PAK1-T109A/K299R. The phosphorylation of the indicated recombinant proteins was visualized using BAS-5000 Bio-imaging Analyzer. These experiments were repeated at least twice with similar results.

similar activity of PAK1 to those infected with Adv-Cre alone (control cells) (Fig. 2*B*). Notably, forced expression of LKB1/STRAD by co-infection of Adv-LKB1 and Adv-Cre decreased the cellular level of the phosphorylated PAK1 but not that of total PAK1 and inhibited the PAK1 activity by ~60% as compared with that in the control cells infected with Adv-Cre or Adv-LKB1 alone (Fig. 2*B*). Furthermore, forced expression of LKB1/STRAD reduced cell migration in MEF3-2 cells (to 35% of Adv-Cre alone) (Fig. 2*C*). To directly test whether LKB1 reduces cell migration through inhibition of PAK1, we infected MEF3-2 cells with various multiplicity of infection of the adenovirus encoding the constitutively active mutant of PAK1 (Adv-PAK1-T423E) together with Adv-Cre/Adv-LKB1. Co-infection with Adv-PAK1-T423E has recovered the LKB1-induced reduction of cell migration in a dose-dependent manner (Fig. 2*C*). These results suggest that LKB1 can contribute to the suppression of cell migration through inhibition of PAK1.

*LKB1 Activity Is Necessary for Suppression of PAK1*—PAK1 can be activated by recruitment of the active forms of Cdc42/Rac and phosphorylation by 3-phosphoinositide-dependent kinase-1 (19). Thus, we investigated whether the protein kinase activity of LKB1 was necessary to suppress the PAK1 activation. HEK293T cells were transiently transfected with PAK1 and/or LKB1/STRAD expression vector to determine PAK1 activity. The wild-type LKB1 (wt) inhibited the activity significantly, whereas the kinase-dead mutant of LKB1 (kinase-dead) did not affect activity (Fig. 3*A*). These results indicated that LKB1 activity was necessary for PAK1 inhibition. Accordingly, we next hypothesized that LKB1-mediated phosphorylation of PAK1 reduced its kinase activity. To test the possibility, we preincubated recombinant PAK1 with various amounts of LKB1 in the presence of ATP and then added the substrate of PAK1 to determine its kinase activity. LKB1 directly inhibited the PAK1 activity *in vitro* in a dose-dependent manner (Fig. 3*B*). These results indicate that LKB1-mediated PAK1 phosphorylation decreases its kinase activity.

*LKB1 Can Phosphorylate PAK1 at Thr$^{109}$*—To study PAK1 phosphorylation by LKB1 further, we searched the LKB1 substrate amino acid sequence motif "LXT" (5, 37) in full-length PAK1. We found an LQT sequence (107–109) within the p21-binding domain (PBD) in the regulatory region located near the N terminus of PAK1 (Fig. 4*A*). To determine whether Thr$^{109}$ of PAK1 could be phosphorylated by LKB1, we constructed a GST-fused PBD recombinant protein (GST-PBD) and its mutated form in PBD, GST-PBD-T109A (Fig. 4*A*). Recombinant LKB1 failed to phosphorylate GST-PBD-T109A *in vitro*, although it phosphorylated GST-PBD efficiently (Fig. 4*B*). Next, we tested whether LKB1 phosphorylated the full-length PAK1 at Thr$^{109}$. To this end, we used a full-length dominant-negative PAK1 recombinant protein (GST-PAK1-K299R) as the substrate to minimize the effect of autophosphorylation and introduced alanine substitution at Thr$^{109}$, GST-PAK1-K299R/T109A (Fig. 4*A*). The full-length PAK1 (GST-PAK1-K299R) was phosphorylated by LKB1 efficiently, whereas the GST-PAK1-K299R/T109A was at a much reduced level (Fig. 4*C*). These results suggest that full-length PAK1 can be a sub-